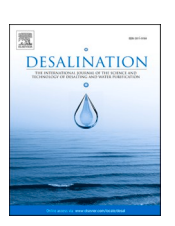


Contents lists available at ScienceDirect

Desalination

journal homepage: www.elsevier.com/locate/desal





An optimization framework for the design of reverse osmosis desalination plants under food-energy-water nexus considerations

Marcello Di Martino a,b, Styliani Avraamidou b, Julie Cook a,b, Efstratios N. Pistikopoulos a,b,*

- ^a Artie McFerrin Department of Chemical Engineering, Texas A&M University, College Station, TX 77843, United States
- b Texas A&M Energy Institute, Texas A&M University, College Station, TX 77843, United States

HIGHLIGHTS

- A superstructure framework for screening of reverse osmosis plant designs is derived.
- The framework enables techno-economic and food-energy-water scenario analysis.
- A surrogate model for the depiction of a reverse osmosis stage is developed.
- The framework is applied to a case study in South-Central Texas.

ARTICLE INFO

Keywords: Reverse osmosis Superstructure representation Optimization Food-energy-water nexus Desalination

ABSTRACT

Due to a growing population, globally depleting water supplies, as well as the effects of climate change, demands for water are ever increasing. Reverse osmosis desalination could play a key role in generating new water sources since treating saline water for reuse has become possible. An optimization based framework under food-energy-water nexus considerations is developed in this work to tackle water scarcity sustainably for arid and semi-arid regions. With the aid of a surrogate model, a single reverse osmosis stage is depicted, with which varying desalination process designs can be composed, considering different membrane modules, as well as varying input energy and saline water sources. Then, the process was modeled through a superstructure representation that resulted into a mixed-integer nonlinear optimization problem, enabling the optimization of an array of objectives for a given set of input water and energy supply, as well as output water demand restrictions. The developed framework facilitates informed decision making through the fast screening and optimization of desalination plant designs. To illustrate the elaborated framework methodology, a food-energy-water nexus approach is implemented for South-Central Texas in three distinct scenario analyses.

1. Introduction

Water scarcity is a severe challenge, especially for arid and semi-arid regions such as Texas [1], California and Baja California [2] or the Middle Eastern Region [3]. With a growing population, not only the water and food demands increase, but also the energy consumption. Since water is traditionally used as a coolant in energy production plants, as well as needed for agriculture and livestock for food production, the water consumption further rises [4,5]. Consequently, water, food, and energy production are linked to each other, which in turn means that these challenges need to be solved by a food-energy-water nexus approach [6,7]. The food-energy-water nexus, which describes the interconnectivity of natural resources, postulates that when

decisions concerning the utilization of one resource, in this case water, are made, other resources, in this case food and energy, are affected and vice versa [8,9]. Thus, leading scientists and policy makers to think about food, energy and water systems as connected and coevolving [10]. Moreover, the food-energy-water nexus not only consists of domains related to water resources research [11], sustainability [12], food-waste management [13] or metropolitan scale water management [14], but also of various other scientific fields like psychology [15], sociology [16] and many more. The interested reader is advised to consult [17–19], as well as [20] for further information relating to the principles, practices, decision-making methods, planning and trade-off analysis for the interdisciplinary treatment of the food-energy-water nexus. Further, existing water supplies, like groundwater aquifer storage

^{*} Corresponding author at: Artie McFerrin Department of Chemical Engineering, Texas A&M University, College Station, TX 77843, United States. E-mail address: stratos@tamu.edu (E.N. Pistikopoulos).

systems, are depleting globally. If the groundwater recharge is exceeded by the groundwater withdrawal for extensive areas and an extensive period of time, overexploitation or persistent groundwater depletion can occur, which can result in devastating effects on natural streamflow, groundwater-fed wetlands and related ecosystems [21].

Additionally, climate change is expected to make water shortages worse: the Intergovernmental Panel on Climate Change (IPCC) projected that up to two billion people worldwide could be facing water shortages by 2050. Moreover, climate change will not only affect water scarcity but also a sustainable water supply by decreasing natural water storage capacity and affecting the capacity and reliability of water supply infrastructure (due to extreme weather or flooding) [22,23]. Therefore, to cope with these upcoming severe challenges, novel water sources are needed [24].

Desalination processes could play a key role in tackling these challenges since treating sea water, surface water, industrial wastewater or brackish water for reuse has become possible [25,26]. A process that removes salts and minerals from a saline water source, for human consumption and domestic or industrial usage, is referred to as desalination [27]. Traditionally, thermal separation methods were used to purify saline water. However, with recent advances in membrane technology, membrane separation methods have become more and more popular, particularly reverse osmosis (RO) desalination processes [26,28]. Reverse osmosis desalination systems have high energy efficiency, low space requirements, as well as process and plant compactness among other advantages in comparison to thermal desalination technology [27]. Consequently, 88% of the desalinated water in the United States is produced by reverse osmosis [29]. This work investigates reverse osmosis process systems, but future extensions could cover other desalination processes.

So far, there have been a variety of distinct optimization analyses concerning reverse osmosis systems, but to our knowledge, a holistic Food-Energy-Water Nexus approach, alternating or rather optimizing the water and energy sources, as well as the membrane system itself, in an attempt to meet the local water demands for varying output water applications, has not yet been investigated, which is the scope of this work. Therefore, data for renewable energy and grid electricity, as well as for seawater, surface water, groundwater, and industrial wastewater, together with reverse osmosis process properties is collected and used for the modeling and simulation of different desalination alternatives that can then be used for optimization. The developed process systems engineering approach for reverse osmosis desalination possibilities dependent on regional factors is summarized in Fig. 1. Grossmann et al.

[30,31] already discussed that process systems engineering (PSE) is uniquely positioned to address the challenges encountered in the sustainability of food-energy-water nexus problems, as well as sustainability problems in general, within chemical engineering and beyond. Within PSE hierarchical decomposition and superstructure synthesis are the two main approaches for conceptual process design, although superstructure synthesis is the preferred alternative, as it has the key advantage of systematic and integrated analysis of alternative process structures [32].

Thus, a superstructure based mathematical model is developed, which has the form of a mixed-integer nonlinear programming (MINLP) problem. The developed model can then be optimized for various scenarios resulting in a plethora of optimal solutions for decision makers, enabling a framework methodology, for the techno-economic and feasibility analysis of desalination plants. Hence, this approach can be used for reliable and fast screening of reverse osmosis plant designs prior to detailed plant modeling.

This work focuses on the Food-Energy-Water Nexus for South-Central Texas (USA), defined as Region L by the Texas Water Development Board (TWDB), but can be easily modified and applied to any given region around the world, underlining the framework nature. Region L is historically rooted in agriculture and contains a growing metropolitan hub with the city of San Antonio. Furthermore, the region is characterized by a finite supply of water resources [8]. Therefore, water management is a key issue for Region L (likewise for the whole state of Texas and other regions with water scarcity challenges). Conventional water management strategies, like conservation or groundwater, are not sufficient for meeting prognosticated demands, resulting in a growing share of technology based water supplies, like reverse osmosis desalination [1].

The population of Region L is expected to reach more than 5 million by 2070, with a water demand projected to increase by 34% [33]. While the total water demand increases, the existing ground water supply of Region L stays approximately constant (expected to increase by 2%) [33]. Consequently, the discrepancy between water demand and supply will rise significantly over the upcoming years. This prognosis underlines that a holistic nexus approach, which considers the interconnectivity of resources like food, energy, and water, is a necessity for tackling these challenges sustainably [8,34].

The water demand projection for various industries, the sum of which gives the total water demand forecast, needs to be evaluated as well. The main water demand drivers are not only municipal water

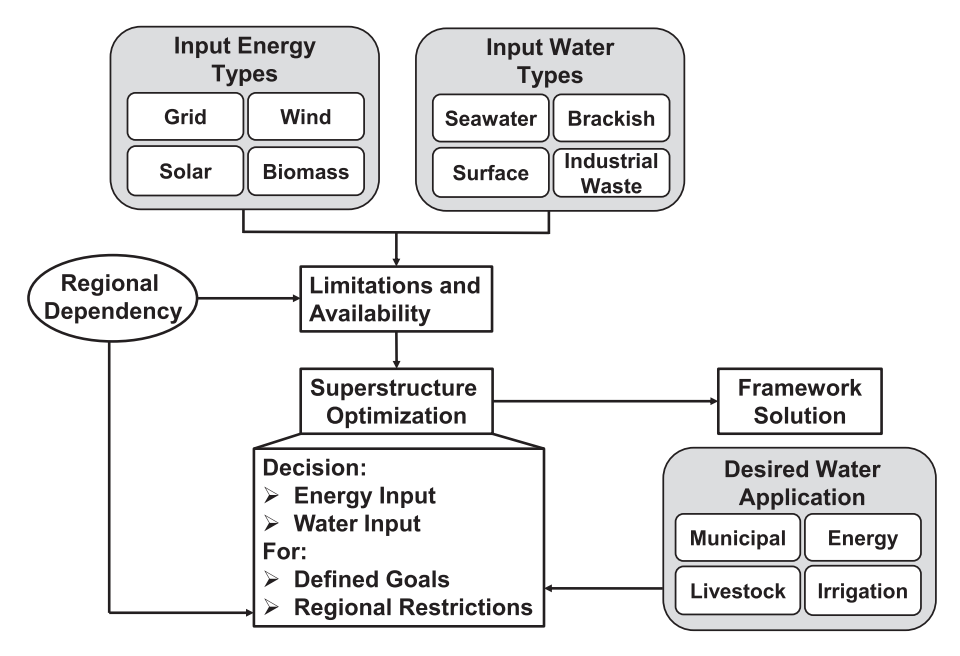


Fig. 1. Summary of the elaborated framework methodology approach.

usage, but also water for irrigation, as well as livestock together with the water demand for steam-electric power, mining and manufacturing [33]. Therefore, output water applications other than municipal water usage need to be considered when tackling reverse osmosis desalination optimization holistically.

Fortunately, Texas is perfectly suited for desalination with more than 360 miles of coastline along the Gulf of Mexico, and more than 30 aquifers spreading across the state, each containing an ample supply of brackish groundwater [1]. Therefore, analyzing different desalination systems holistically for various energy and water inputs is necessary to assess the possibilities and limitations of desalination systems, evaluate food-energy-water nexus trade-offs and identify optimal cost-effective and sustainable desalination plant designs. A novel framework for the optimal design of desalination process plants is developed and presented in this work as a means of tackling the water scarcity in water-stressed regions such as Texas. Furthermore, the proposed approach is easily applicable to other regions around the globe facing water scarcity.

After a brief literature review that comprises advances in the optimization of desalination systems as well as advances in RO optimization with and without food-energy-water nexus considerations, the superstructure representation of the reverse osmosis desalination system is described. Then, the single-stage reverse osmosis surrogate model is derived and used to compose a multi-stage process, depending on the total dissolved solids concentration of the input water source. Subsequently, the energy optimization model, which is used for deriving electricity prices, is defined. Before applying the optimization framework to a threefold case study of South-Central Texas, the optimization model itself, together with the solution methodology are stated.

2. Literature review

In recent years, publications addressing, summarizing or reviewing advances in RO technology and processes have been released regularly, e. g. [27,35]. In these cases, either an overview of advancements in systematic optimization of the design and operation of water desalination, together with a summary of techniques and optimization tools that have been applied to desalination processes for design and/or operation purposes of said processes are given [35], or distinct aspects of reverse osmosis processes are reviewed, such as studies related to membrane modules, characterization, fouling and cleaning, different pre-treatment technologies, principles of RO process designs including the embedded economy, as well as energy considerations, together with hybrid RO process designs and current challenges faced by RO desalination processes [27]. Additionally, there has been an opulence of work concerning desalination process optimization, particularly regarding reverse osmosis processes, without food-energy-water nexus considerations.

Generally, RO optimization has been studied with a focus on key aspects of the desalination process: Kotb et al. [36] analyzed and optimized the RO desalination system arrangement, as well as operating conditions. Al-Obaidi et al. [37] evaluated the performance of a multistage RO wastewater treatment system considering a number of alternative configurations with recycling of permeate, retentate, and permeate-retentate streams. Ghobeity et al. [38] optimized timedependently the operation of a seawater desalination process. Zhu et al. [39] optimized the energy consumption of a RO process prone to feed water salinity fluctuations. In addition, RO processes only powered by solar energy haven been simulated and optimized with the aim of enhancing the recovery rate and product quality of the system, while operational limits of the system are reduced [40]. Hybrid desalination processes have been under investigation as well, e.g. Ghobeity et al. [41] developed a conceptual design and system-level models of a cogeneration solar-thermal plant, whose operating conditions have been subsequently optimized. In contrast, Sadri et al. [42] determined the best trade-off between the exergetic efficiencies of multi-effect desalination (MED) and RO, which led to the selection of a hybrid MED-RO system. Additionally, Al-hotmani et al. [43] studied a hybrid system of multi effect distillation thermal vapor compression and reverse osmosis, for seawater desalination. To take into account increasing water demands, the permeate reprocessing design of the RO process is introduced in several configuration of different upstream processes.

Different types of optimization approaches for desalination systems has already been studied. Saif et al. [44] developed a deterministic branch-and-bound global optimization-based algorithm for the solution of the reverse osmosis network synthesis problem. In this case, to illustrate the global optimization of the RO network, water desalination is considered as a case study. Du et al. [45] investigated RO networks for seawater desalination with spiral-wound membrane modules. After comparing the model results with actual operational plant data from the literature, the optimum design problem was formulated as a MINLP problem and solved. Subsequently, Du et al. (2014) [46] extended their study to multi-objective optimization, using the ∈-constraint method, to investigate the trade-off between total annualized cost, energy consumption and the recovery rate of the process. Khor et al. [47] developed a detailed model representation for water regeneration network synthesis, in which nonlinear mechanistic models of the regeneration units are embedded within an overall MINLP optimization framework, which is then used for an illustrative industrial case study of an operating refinery in Malaysia. The results indicate the possibility of 58% freshwater savings. Sassi et al. [48] focused on a MINLP optimization framework for boron removal in RO desalination systems. The approach includes a seawater pass containing a normal two-stage RO system housing seawater membrane modules and a brackish water pass accommodating brackish water membrane modules.

All mentioned studies have in common that they do not address the food-energy-water nexus holistically, but rather focus on principal challenges for distinct scenarios. Although, the overall water demand of arid and semi-arid regions not only consists of municipal water usage but also of the water consumption of other industries like livestock, irrigation or power generation [33], usually only one specific water output application, mostly for drinking purposes, has been considered in optimization studies of RO processes.

Lately, RO desalination optimization with food-energy-water nexus reflections has become more and more common. For example, Gabriel et al. [49] reviewed and optimized a hybrid RO system coupled with industrial processes exhibiting a net surplus of heat energy. Li [50] optimized a multi-stage hybrid RO-PRO (pressure retarded osmosis) membrane process to address the energy-water nexus. Al-Aboosi et al. [51] developed a design framework for integrating water and energy systems, a cogeneration process and desalination technologies, to treat wastewater and provide fresh water for shale gas production. Linke et al. [52] visualized the trade-offs between the minimum total annual cost and environmental sustainability metrics of industrial water networks. Additionally, Al-Mohannadi et al. [53] maximized carbon reduction, as well as economic performance of a defined industrial cluster containing e.g. oil refinery, steel production and natural gas fired power plants among other sources and sinks, using a multi-objective multi-period optimization tool. Again, comparable to RO optimization studies without nexus considerations, these exemplary studies focus on key parts and challenges of reverse osmosis desalination processes to address the interconnectivity of energy and water resources.

A review by Vakilifard et al. [54], which addresses the role of the energy-water nexus in optimizing water supply systems, has identified a lack of studies attempting to optimize the energy-water nexus holistically. Also, optimization frameworks with the possibility of incorporating environmental impact studies were deemed to be virtually nonexistent. Moreover, the water demand or rather the impact on a water supply scenario by the food industry is frequently not taken into consideration when talking about nexus solutions or optimization studies.

Since the development of new processes and technologies is more and more driven by sustainable criteria [55], the goal of the here elaborated reverse osmosis desalination optimization framework is to develop an integrated methodology, which facilitates incorporating

environmental impact studies of solution strategies, while simultaneously addressing the food-energy-water nexus holistically. The potential of desalination alternatives can be assessed for varying supply and demand scenarios, while further restrictions or goals, as the environmental impact of process solutions, can be considered, in an attempt to initially, partially fill the research void concerning reverse osmosis desalination optimization studies addressing the food-energy-water nexus identified by Vakilifard et al. [54].

3. Superstructure representation

The intent of this work is to address the design of reverse osmosis desalination processes holistically in terms of the input water types, the energy sources, the membrane types, as well as the process operation and parameters, for various output goals and output water applications. The goals considered do not only include maximizing revenue or minimizing cost, but also satisfying a given water demand for different output water characteristics (like municipal, irrigation, livestock or power plant usage), or minimizing environmental stresses. Thus, the food-energywater nexus is incorporated in the approach, through varying application possibilities, considering water and energy resources for defined output utilizations like the food industry. Consequently, the framework can be used in food application processes to incorporate the interconnectivity of food, energy and water. A summary of these considerations is given in Fig. 2. The framework is modifiable for any given region by adjusting restrictions concerning water and energy, emphasizing the framework methodology nature of the implemented approach. A schematic representation of the developed superstructure can be found in Fig. 3. The superstructure can be subsequently expressed in a mathematical model, which has the form of a MINLP problem.

The RO desalination framework is derived in the following steps:

- 1. A mathematical model to describe a single-stage reverse osmosis process is developed (Section 4 and 1.1–1.3 of the supplementary file), with which a multi-stage process can be configured (Section 1.4 of the supplementary file).
- The optimization program for decision making concerning the usage of available energy sources is elaborated (Section 2 of the supplementary file).
- 3. The equations governing the design optimization problem are presented and discussed (Section 5), before introducing the used solution strategy (Section 6).

Then, the derived model is used for case studies in South-Central Texas to analyze the potential and applicability of the derived model (Section 7).

4. Development of the reverse osmosis model

A schematic representation of a one-stage reverse osmosis process,

Energy
Sources

Renewable

Grid
Electricity

Hybrid

Input Water
Types

Seawater

Brackish
Industrial
Waste

Surface

together with the variables describing it is illustrated in Fig. 4. A feed stream with volume flow Q_f and concentration C_f is pressurized to a pressure P_f , so that separation of the saline feed into a diluted permeate (Q_p, C_p, P_p) and a concentrated retentate (Q_r, C_r, P_r) can be achieved in the reverse osmosis membrane module. Membrane modeling is classically used to calculate the necessary pressurization of the feed streams for a certain permeate concentration quality (or vice versa) since the pressurization is the main energy cost driver of the system [56].

To calculate the specific energy consumption of the pump pressurizing the feed, the transmembrane pressure needs to be calculated ($\Delta P = P_f - P_p$) together with the feed and permeate volume flow [m³/d] (see Eq. (1)), while also considering the pump efficiency η [57].

$$SEC_{pump} = \frac{Q_f \cdot \Delta P}{\eta \cdot Q_p} \tag{1}$$

In Eq. (1) the reciprocal of $\frac{Q_p}{Q_j}$ can be found. This fraction is also called the water recovery of the process [24].

To further define the volume flows and the transmembrane pressure, a mass balance and a component mass balance is derived (Eqs. (2) and (3)) [58]:

$$Q_f = Q_p + Q_r \tag{2}$$

$$Q_f \cdot C_f = Q_p \cdot C_p + Q_r \cdot C_r \tag{3}$$

The permeate volume flow can also be expressed in terms of the membrane surface area A in $[m^2]$ and the membrane water flux J_v in [m/s] [27]:

$$Q_p = A \cdot J_v \tag{4}$$

Additionally, it is possible to use the water J_{ν} and salt flux J_{s} , to define the permeate concentration [36]:

$$J_s = J_v \cdot C_n \tag{5}$$

The water flux is typically proportional to the net pressure driving force across the membrane ($\Delta P - \Delta \Pi$, transmembrane pressure difference minus osmotic pressure difference of the feed and permeate side), whereas the salt flux is defined by the amount of salt passing through a unit membrane surface area per unit time, which is proportional to the salt concentration difference across the membrane [27].

However, these equations are not yet sufficient to fully describe the membrane system. To further investigate the mass transfer principles around a reverse osmosis membrane, the Film Theory can be consulted, which takes the concentration polarization phenomenon on the feed membrane side into account [59]:

$$\frac{C_w - C_p}{C_b - C_p} = exp\left(\frac{J_v}{k}\right) \tag{6}$$

Here C_w denotes the salt concentration at the membrane surface, whereas C_b gives the salt concentration in the bulk solution. $k=\frac{\delta_f}{D}$ is the

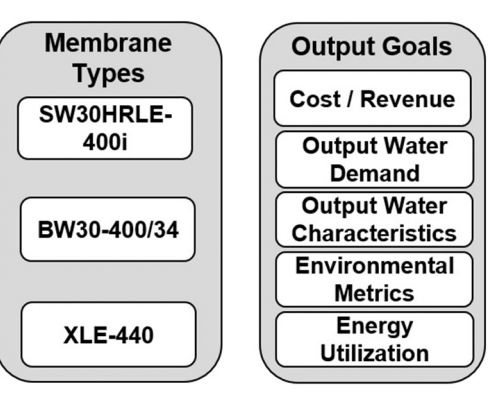


Fig. 2. RO desalination optimization framework considerations.

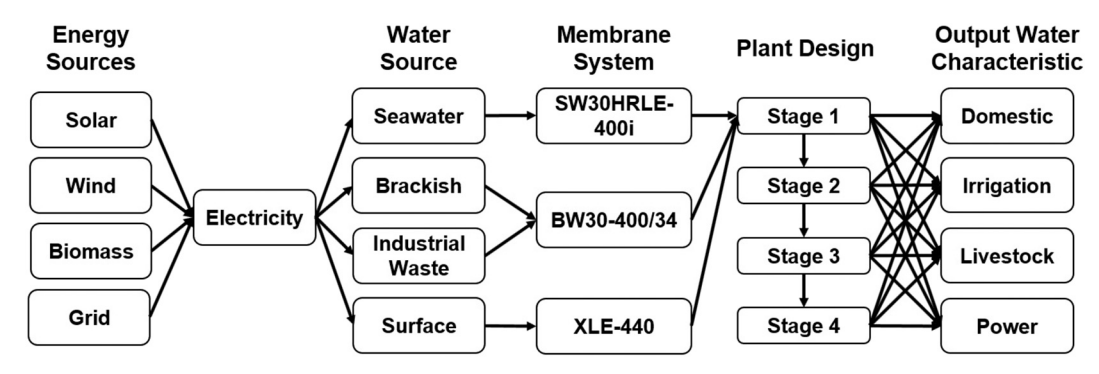


Fig. 3. RO desalination superstructure representation.

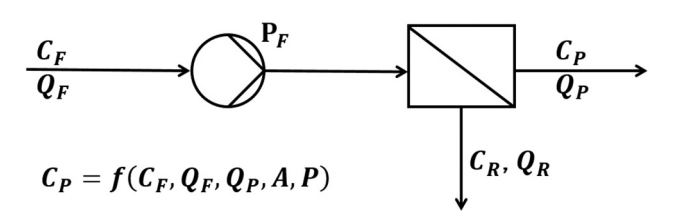


Fig. 4. A schematic representation of a one-stage membrane process.

convective mass transfer coefficient, which needs to be calculated by a convective mass transfer correlation. The Film Theory is presented in detail in [27,36].

Further, all equations mentioned above are summarized in the so called solution-diffusion model [60], which has been shown to adequately predict the local behavior and performance of high rejection membranes such as reverse osmosis membranes [61]. Using the solution-diffusion model for membrane modeling as part of an optimization problem results in a highly nonlinear non-convex programming problem. Since integer decisions additionally need to be incorporated for design decisions, solving the generated optimization program will take a lot of computational effort [62]. Besides, in order to use the solution-diffusion model, access to the exact membrane geometry and flow conditions for the convective mass transfer correlations is needed. To overcome these challenges, a membrane supplier software was used, which takes into account the solution-diffusion model to generate inputoutput data, which can then be approximated by a multivariate linear regression, resulting in a reduction of computational effort [63].

This multivariate linear regression yields an approximation of a single stage RO unit and can subsequently be used to compose a RO desalination process with varying flow structures. Furthermore, a decision between various available energy sources and used generating technologies is enforced by minimizing the sum of operational and investment costs of each alternative with the aim of satisfying a given yearly energy demand. The details of both approaches are specified in Sections 1 and 2 of the supplementary file of this publication, as well as in Table 6 and 7 of Appendix A.

5. Design optimization

$$\min_{x,n,w} f(x,n,w) \tag{7a}$$

$$\sum_{i=1}^{n} m_{i,j} \cdot Q_{p,i,j} = Q_{p,sum,j} \qquad \forall j = 1, ..., w,$$
(7b)

$$\sum_{i=1}^{n} m_{i,j} \cdot Q_{p,i,j} = Q_{p,sum,j} \qquad \forall j = 1, ..., w,$$

$$\frac{\sum_{i=1}^{n} C_{p,i,j} Q_{p,i,j} \cdot m_{i,j}}{Q_{p,sum,j}} = C_{p,sum,j} \quad \forall j = 1, ..., w,$$

$$(7b)$$

$$\frac{Q_{p,sum,j}}{Q_{f,1,j}} = WR_{sum,j} \qquad \forall j = 1, ..., w,$$
(7d)

$$C_{f,1,i} = C_{water,i} \qquad \forall j = 1, ..., w, \tag{7e}$$

$$C_{p,sum,j} \le C_{p,restriction}$$
 $\forall j = 1, ..., w,$ (7f)

$$WR_{sum,j} \ge WR_{restriction,j}$$
 $\forall j = 1, ..., w,$ (7g)

$$Q_{n,sum,i} > Q_{n,demand} \qquad \forall i = 1, ..., w, \tag{7h}$$

$$n_j \in \{1, 2, 3, 4\}$$
 $\forall j = 1, ..., w,$ (7i)

$$n \in \mathbb{N}, \qquad \qquad N = \{n_1, \dots, n_{\scriptscriptstyle W}\}, \tag{7j}$$

$$j \in J,$$
 $J = \{1, ..., w\},$ (7k)

The design optimization problem is summarized in (Eqs. (7a)–(7k)). After explaining the governing equations, possible objective functions f(x,n,w) are stated. The objective function f(x,n,w) is not only dependent on the degrees of freedom (DOF) x and the number of stages n, but also on the available water sources w. Here, x consists of the overall feed flow per water source $(Q_{f,l,i})$, the water recovery $(WR_{i,i})$, the pressurization $(P_{i,i})$, the membrane surface area $(A_{i,i})$ and the parallel flows $(m_{i,i})$ per stage i and water source j, for i=1,...,n and j=1,...,w (the length of x is dependent on *n* and *w*), resulting in a number of degrees of freedom of $x = w \cdot (4 \cdot n + 1)$

The DOF are all box-constrained optimization variables. The maximum allowable pressure for each membrane depending on the input water is used as an upper boundary for the pressurization, while the lower boundary ensures applicability and water transport to the membrane. It is important to mention that $P_{i,j}$ describes the necessary pressurization of stage i for water source j to generate the required transmembrane pressure for the separation. The permeate pressure, which is needed for transporting the purified water away from the reverse osmosis module $(P_{p,i,j})$, is also included in the pressurization of stage i ($P_{f, i, j} = P_{i, j} + P_{p, i, j}$) to ensure transport to the membrane, ultimately resulting in:

$$\Delta P_{i,j} = P_{f,i,j} - P_{p,i,j} = P_{i,j}, \quad \forall i = 1,..,n, \quad \forall j = 1,..,w.$$

When a membrane surface area range is implemented, a membrane budget is indirectly considered. Not more than 100 membranes per stage are allowed to be used (to compare: the H2Oaks Desalination plant in San Antonio uses 70 membranes in the first stage of their brackish water desalination process [64]). The boundaries concerning the overall feed flow and water recovery ensure operability and can be modified from scenario to scenario. The design optimization variable $m_{i,j}$ is introduced to account for parallel flows for each stage i and water type j to take higher feed volume flows and water demands into consideration and is limited to five, but can be adjusted if necessary.

Beginning with the overall feed $(Q_{f,1,j})$, the parallel flows per stage (m_1,j) and the water recovery of the first stage $(WR_{1,j})$, the permeate flow of the first stage is calculated $(Q_{p,1,j})$, before using the surrogate model to determine the permeate concentration of the first stage $(C_{p,1,j})$. After closing the mass and component mass balances, the retentate of the first stage $(Q_{r,1,j})$ and $(Q_{r,1,j})$ is redefined as the feed flow for the second stage $(Q_{f,2,j})$ and $(Q_{f,2,j})$. This procedure is continued until all stages $(Q_{f,2,j})$ are determined. For each stage and water type, the feed flow is divided by $(Q_{f,2,j})$ to calculate a single stage membrane process (surrogate model applicability). Afterward, the permeate flow as well as the retentate flow are multiplied by $(Q_{f,2,j})$ to calculate the overall stage flows and concentrations. For seawater desalination processes, the feed of a stage is either defined as the permeate of the previous stage (for stage two) or as the retentate of the previous stage (for stages three and four).

According to the aforementioned process structures, the mass and component mass balances are formulated for each stage i and water source *j* and subsequently used for the definition of a successive stage, although the equations are not shown in Eqs. (7a)-(7k). Once all desalination stages are evaluated, the overall permeate flow $(Q_{p,sum,j}, \text{ see Eq.})$ 7b), permeate concentration ($C_{p,sum,j}$, see Eq. 7c) and water recovery $(WR_{sum.i})$, see Eq. 7d) for each water source j are calculated. These equations need to be adjusted when seawater is used as an available water source, according to the aforementioned seawater desalination process structure. Additional restrictions include an upper boundary for $C_{p,sum,j}$ (depending on the desired water quality output, see Eq. 7f), as well as two lower boundaries for $WR_{sum,j}$ and $Q_{p,sum,j}$ (to ensure a distinct water demand can be met, see Eq. 7g and Eq. 7h). These boundary values are either dependent on the input water source or on the specific scenario. Also, the feed water concentration ($C_{f,1,i}$, see Eq. 7e) is set to the input water type concentration value under investigation ($C_{water,i}$).

Furthermore, model specific restrictions need to be enforced to guarantee the feasibility of the surrogate model. Since the generated data points cannot cover the whole applicable value space, linear interpolation concerning the feed concentration and water recovery is used to extend the model.

Consequently, the following restrictions are enforced for brackish water reverse osmosis processes, to ensure that the brackish water case stays valid (see Eqs. (8) and (9)):

$$C_{r,i,j} \le 10000 \,\mathrm{mg/L} \quad \forall i = 1, ..., n-1, \quad \forall j = 1, ..., w$$
 (8)

$$C_{r,n-1,j} \ge 700 \,\text{mg/L} \quad \forall j = 1,..,w$$
 (9)

The mentioned restrictions need to be adjusted accordingly to guarantee feasibility in the case of seawater desalination processes. For a two-stage seawater reverse osmosis process, it is practical to force the permeate of the first stage to be less than 10,000 mg/L so that interpolation between seawater and brackish water membrane data is not necessary (see Eq. (10)):

$$C_{p,1,j} \le 10000 \,\mathrm{mg/L} \quad \forall j = 1,..,w$$
 (10)

Additionally, the following restrictions are necessary for a three- and four-stage seawater reverse osmosis process, respectively (see Eqs. (11) and (12) for three stages and Eqs. (11), (13) and (14) for four stages):

$$C_{r,2,j} \le 10000 \,\mathrm{mg/L} \quad \forall j = 1,..,w$$
 (11)

$$C_{r,2,j} \ge 700 \,\text{mg/L} \quad \forall j = 1,..,w$$
 (12)

$$C_{r,3,j} \le 10000 \,\mathrm{mg/L} \quad \forall j = 1,..,w$$
 (13)

$$C_{r,3,j} \ge 700 \,\text{mg/L} \quad \forall j = 1,..,w$$
 (14)

Consequently, this results in a process scheme which uses a seawater membrane for the first stage and brackish water membranes in subsequent stages.

5.1. Objective functions

A variety of objective functions can be considered within the proposed framework. Approaches for maximizing the water recovery, minimizing the energy, as well as minimizing operational costs are presented in this work.

Maximizing the water recovery for a given water source j is presented in Eq. (15):

$$f(x,n,w)_1 = -\frac{Q_{p,sum,j}}{Q_{f,1,j}} = -\frac{\sum_{i=1}^n m_{i,j} \cdot Q_{p,i,j}}{Q_{f,1,j}}$$
(15)

To maximize the overall water recovery (Eq. (15)), the negative fraction of the overall permeate $(\sum_{i=1}^n m_{i,j} \cdot Q_{p,i,j})$ and overall feed $(Q_{f,1,j})$ is minimized.

For minimizing the energy of the system for a given water source *j*, the specific energy consumption of the pumps as well as possible energy recovery devices need to be considered (see Eq. (16)) [39]:

$$f(x, n, w)_{2} = \sum_{i=1}^{n} \left(\frac{Q_{f,nec,i,j} \cdot P_{nec,i,j}}{\eta_{pump}} - \eta_{ERD} \cdot Q_{res,i,j} \cdot P_{res,i,j} \right)$$
(16)

In Eq. (16), η_{pump} and η_{ERD} take the pump efficiency as well as the efficiency of the ERD into account. $P_{nec,i,j}$ describes the necessary pressurization of a stage and is set to 0 if the residual pressure of a previous stage is sufficiently high to be used in a subsequent stage. Accordingly, $Q_{f,nec,i,j}$ incorporates the feed flows of stages where pressurization is needed. In contrast, $P_{res,i,j}$ is a vector of pressure differences that can be used for energy recovery, if the pressure of the retentate is higher than the necessary transmembrane pressure of the successive stage (these differences are then added to $P_{res,i,j}$). The retentate flows are saved in $Q_{res,i,j}$ accordingly. Thus, $f(x,n,w)_2$ is calculated in [MW].

The main portion of operating costs of reverse osmosis desalination systems is constituted by energy costs ($C_{E,j}$) [35]. The only additional factors that contribute significantly to operational costs are brine concentrate disposal costs ($C_{B,j}$) as well as membrane costs ($C_{M,j}$). Therefore, operational costs of a desalination system using an input water source j are assumed to only consist of the aforementioned three components (Eqs. (17) to (20)).

$$f(x,n,w)_3 = C_{E,j} + C_{B,j} + C_{M,j}$$
(17)

$$C_{E,j} = e_c \frac{f(x, n, w)_2}{Q_{n, vam, i}}$$
(18)

The energy cost factor e_c (Eq. (18)) is dependent on the energy supply system (see section energy optimization model in the supplementary material). By dividing $e_c \cdot f(x, n, w)_2$ by $Q_{p,sum,j}$, the energy costs $\left[\frac{s}{m^3}\right]$ are calculated on the basis of the permeate volume flow.

$$C_{B,j} = b_{c,j} \cdot \left(\frac{C_{f,1,j} - 1000}{35000 - 1000} \cdot 100 \cdot \left(\frac{1 - WR_{sum,j}}{WR_{sum,i}} \right) \right)$$
 (19)

The brine cost function (Eq. (19)) was obtained from [39], where the fraction $\frac{1-WR_{sum,j}}{WR_{sum,j}}$ can also be expressed as $\frac{Q_{r,sum,j}}{Q_{p,sum,j}}$. Additionally, a linear approximation $\left(\frac{C_{f,1,j}-1000}{35000-1000}\cdot 100\right)$ was used to incorporate the brine management cost (defined as $\frac{b}{II_0}$ by [39], where b is the brine management cost and Π_0 the osmotic pressure of the feed). For example, a feed concentration of 1000 mg/L has a dimensionless brine management cost of 0, whereas a feed concentration of 35,000 mg/L has a dimensionless brine management cost of 100. Further, an additional factor of $b_{c,j}$ in $[\$/m^3]$ is introduced to scale the brine management costs and has changing values dependent on the water source (see section Model assumptions). Consequently, $C_{B,j}$ is in $\left[\frac{\$}{m^3}\right]$.

$$C_{M,j} = \frac{me_{c,j} \cdot N_{m,j} + \nu_{c,j} \cdot N_{v,j} + \left(R_{v,j} \cdot \frac{\nu_{c,j} - \nu_{v,one,c,j}}{7 - 1} + n_j\right)}{(LS/365/24) \cdot Q_{p,sum,i}}$$
(20)

The membrane costs (Eq. (20)) consist of the membrane purchase costs as well as the pressure vessel purchase costs. The number of membranes $N_{m,j}$ is calculated by dividing the total membrane surface area $(\sum_{i=1}^{n} m_{i,j} \cdot A_{i,j}, \forall j=1,...,w)$ by the area of a single membrane (37 m² for all three membrane types). $N_{m,j}$ is divided by 7 (maximum of 7 membranes in one pressure vessel), to calculate the overall number of pressure vessels $(N_{\nu,i})$. It may occur that the last pressure vessel per stage is only partially filled with membranes. In this case, a pressure vessel, which has room for 7 membrane units, is not needed as the last pressure vessel of the stage, since a smaller one can be selected. This is considered with $(R_{\nu,j}, \frac{v_{c,j}-v_{\nu,one,c,j}}{7-1} + n_j)$, where $R_{\nu,j}$ is the remainder of the fraction $\frac{N_{m,j}}{7}$. The prices of membranes $me_{c,j}$, pressure vessels $v_{c,j}$ and the correlation $(R_{\nu,i} \cdot \frac{v_{c,j} - v_{\nu,one,c,j}}{7.1} + n_i)$ are summarized in the section Model assumptions. Additionally, the stated costs are divided by the assumed membrane lifetime LS in [years] as well as the overall permeate flow, resulting in a membrane cost unit of $\left[\frac{\$}{m^3}\right]$.

5.2. Model assumptions

The previously defined design model (Eqs. (7a)–(7k)) is only focusing on the reverse osmosis separation unit itself. Moreover, it is assumed that the feed water of the desalination unit is pretreated by ultrafiltration (defined in WAVE for the data generation for the surrogate model), making sure that only dissolved solids are left to be separated from the feed water stream. Consequently, the model does not consider membrane cleaning or fouling, since these factors strongly depend on the used pretreatment unit and its operation quality [65], which is not considered in detail.

Concerning the permeate pressure no numerical assumption is necessary, since the transmembrane pressure has been selected as a decision variable. It is assumed that the needed pressure for transportation to the membrane on the feed side and the needed pressure for transportation away from the membrane of the permeate side are equal and thus cancel out when focusing on the transmembrane pressure.

An additional assumption is that the desalination plant is operated in steady-state, although practically fluctuations in input parameters occur regularly (e.g. concerning the feed volume flow), which are noticeable but not significant for the process design. Further, ramping up and down a given desalination plant from distinct capacities (from 0 to 1 excluded; 0: plant is not running; 1: plant is operated at maximum capacity, capacity = $\frac{Q_{f,operation}}{Q_{f,macpossible}}$) is not challenging [64]. However, since for a reverse osmosis desalination unit control strategies can be easily implemented, a quasi-stationary process can be enforced [27]. Therefore, the assumption of steady-state is not too strict and still applicable.

Furthermore, assumptions concerning the energy and operational cost objective functions have been made:

- 1. The efficiencies of the pump as well as of the ERD are constant ($\eta_{pump} = 0.74$ and $\eta_{ERD} = 0.8$) [66].
- 2. The average membrane life is assumed to be 7 years. The membrane lifetime depends on the pretreatment and is usually between 3 and 5 years but can also last up to 15 years [67].
- 3. A brine cost parameter b_{c,j} has been introduced in the brine cost function, which is 0.2\$/m³ for brackish water applications [39] and 0.05\$/m³ for seawater applications [68]. Additionally, the stated brine cost correlation can be updated for any specific application and region. The given function is used to illustrate the process implications of brine disposal, more specifically, to penalize low water recoveries due to the scarcity of water and high value of available water sources in arid and semi-arid regions, to reduce process water waste reasonably.

 Investment costs are not considered. Here, decisions are only made based on maximizing water recovery, minimizing energy consumption or operational cost minimization.

An overview of the membrane costs and membrane pressure vessel costs can be found in Table 8 in Appendix A. High-pressure pressure vessels can withstand a pressure of up to 83 bar, whereas low-pressure pressure vessels can tolerate a pressure of only 31 bar.

Moreover, the stated assumptions can be subsequently investigated by performing sensitivity analyses. The assumed membrane lifetime (LS), as well as the brine cost parameter $b_{c,j}$ of the brine cost function, have been selected respectively for a sensitivity analysis, which can be found in the supplementary file.

6. Solution methodology

The stated design optimization model, as well as the surrogate model, have been implemented in MATLAB. An overview of the framework solution methodology can be found in Fig. 5.

First of all, a problem needs to be defined in the sense that the available water (total dissolved solids concentrations and possible daily volume flows) and energy sources (cost of each energy source) need to be specified. Secondly, all available water sources are summarized in J=1,...,w.

Now, the counting variable $j \in J$ is initialized to one (j = 1), to evaluate the first water source. Then, design optimization is performed, which includes the number of stages and the number of parallel flows $(m_{i,j})$ as integer variables. The integer variable number of stages n is always limited to four $(1 \le n_j \le 4, \forall j \in J)$, so a brute-force approach is selected to determine the optimal number of stages for a desalination process using water source $j \in J$. However, because of the integer variable $m_{i,j}$, the resulting optimization problem is a MINLP problem.

The resulting MINLP problems with nonlinear inequality constraints were solved with the genetic algorithm introduced by Deep et al. for integer and mixed-integer optimization problems [69]. The best solution is then saved before checking if other water sources are still to be evaluated. If this is the case (j < length(J)), the counting variable is adjusted (j = length(J))j + 1) and the same optimization is performed for the next water source. Once all water sources are evaluated, all solutions are compared and the best one is selected. Since there is always only a finite and comparably small number of water sources (e.g. no more than five) for each water scarce region, binary decision variables for each water source are obsolete and only cost additional computational effort. Additionally, the least saline water source is always the cheapest option concerning operational cost because of the lower necessary pressures throughout the system. Once a water demand cannot be satisfied with the lowest saline water source, the next higher saline water source is selected until this water source cannot fulfill a given demand anymore and so on.

For all calculated and presented cases a local minimum was found, which satisfies the determined constraints. Global optimality cannot be guaranteed when using the genetic algorithm. Although by using a global MINLP solver such as ANTIGONE [70] or BARON [71] global optimality could be guaranteed, it is at this point not necessary, as this methodology is used to make a first assessment of available water and energy sources for desalination. Therefore, the goal of the developed holistic process systems approach of desalination processes is to point decision makers in the right direction to help evaluate which cases should be investigated in a more detailed fashion and which not.

If no parallel flows per stage are to be considered, the optimization problem is reduced to a non-linear program (NLP) by brute forcing the number of stages n. Consequently, an interior-point solution algorithm can be used for solving the optimization problem. The interior-point algorithm was selected to guarantee feasibility since all iterates are required to satisfy the inequality constraints of the problem strictly [62]. The NLP is here called operation optimization and is used for determining possible process flow structures for varying water sources (see

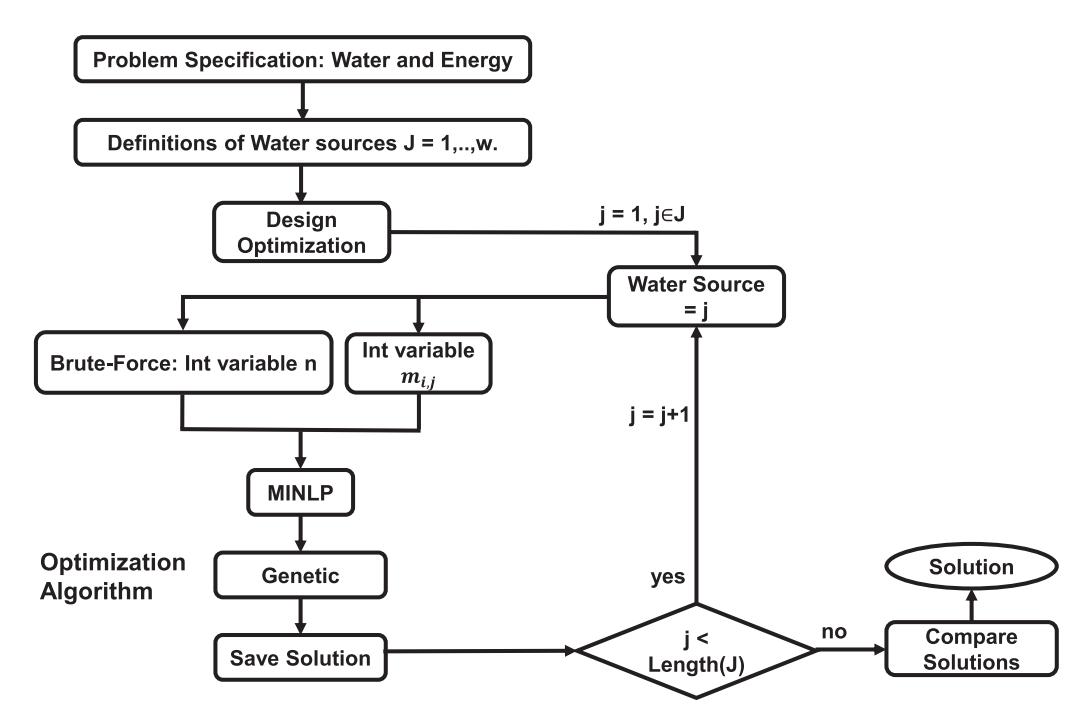


Fig. 5. Schematic illustration of the framework solution methodology.

supplementary file), in addition to performing sensitivity analyses concerning the membrane lifespan and the brine cost function parameter (see supplementary file).

7. Case study region L (South-Central Texas)

Before analyzing three exemplary water supply scenarios, each addressing another aspect of the food-energy-water nexus (municipal usage, irrigation, power generation), the available water sources and water restrictions for Region L are stated.

7.1. Available water sources and restrictions

An overview of possible input water types for the desalination design optimization framework of Region L defined by the TWDB can be found in Appendix A, Table 9. The specified TDS concentrations (Table 9 in Appendix A) are used to define $C_{water,j}$ of the design optimization program.

With these different input water sources, various output water characteristics can be achieved by applying a reverse osmosis desalination process. A summary of possible output water restrictions and applications is given in Table 1. Municipal, irrigation, livestock and steam electric power are major water demand applications and are therefore the only applications considered in this work [33,72].

The dissolved solids concentration restrictions specified in Table 1 are used to define $C_{p,restriction}$ for design optimization. Hence, all input and output water types are well defined. If the framework methodology should be applied to another region around the globe, the input water definitions and output water restrictions need to be updated accordingly.

Table 1Desalination output water characteristics depending on application.

Water application	Permeate restriction	Source
Drinking water	$C_{p,sum} \leq 500 \text{ mg/L}$	[73]
Irrigation	$C_{p,sum} \leq 600 \text{ mg/L}$	[73,74]
Livestock	$C_{p,sum} \leq 1000 \text{ mg/L}$	[73]
Power plant	$C_{p,sum} \leq 2500 \; ext{mg/L}$	[75]

7.2. Scenarios

As stated in Section 1, there is an increasing discrepancy between the water supply and the water demand forecast [33]. Therefore, there is not only a desire for minimizing operational costs but also to maximize the generated permeate flow of desalination systems. In the following, the developed methodology is used to analyze and optimize three different case studies to evaluate these competing process objectives:

- 1. Drinking water: The energy supply for a municipal water demand scenario needs to be satisfied with a combination of grid electricity and renewable energy sources. The competing objectives minimizing operational costs and maximizing permeate flow are assessed for varying fractions of grid electricity to renewable energy, so that an environmental metric, like penalizing energy sources which emit carbon, with the goal of minimizing carbon emissions, can be indirectly considered.
- Water for irrigation: Seawater, aquifer water, and surface water are used to analyze the trade-off between minimizing costs and maximizing increasing output water demands for irrigation purposes. The energy for the desalination process is supplied by grid electricity.
- 3. Water for power generation: Only seawater is used to fulfill a specific power generation water demand. Firstly, the design of the desalination plant is determined when only grid electricity is used. Secondly, the same optimization will be performed, but now only solar and wind energy are available energy supply sources.

7.2.1. Scenario I: drinking water

The energy supply for the desalination process consists of a combination of renewable energy sources and grid electricity. Pareto Front for various grid electricity to renewable energy fractions are created to capture the impact of an environmental metric on the solution of competing objectives like maximizing the permeate flow and minimizing the operational costs. The changing energy supply fraction results in varying energy cost factors e_c and therefore directly influences the operational costs. Exemplary environmental metrics can incorporate penalizing carbon based energy production or rewarding renewable energy sources.

In this case, industrial wastewater from a semi-conductor manufacturer in San Antonio is used as input water (C_f , 1, j=5600 mg/L and Q_f , 1, $1 \le 12500$ m³/d). Additionally, the permeate flow is restricted to be at least Q_p , S_0 , S_0 , S_0 , S_0 , resulting in a water recovery of S_0 , S_0 , S_0 , initially, the stated specifications were used with S_0 escapable energies only, for details see Scenario III) to determine an energy output range for the energy optimization model by minimizing the energy and the operational cost.

Minimizing the energy of the system results in a three-stage process ($WR_{sum,\ j}$ =78.57%, $Q_{p,\ sum,\ j}$ =8750 m³/d) with an energy demand of 0.2112 MW and operational cost of 0.8022\$/m³ ($C_{E,\ j}$ =0.0174\$/m³, $C_{B,\ j}$ =0.7379\$/m³, $C_{M,\ j}$ =0.0469\$/m³). In contrast, minimizing operational costs yields an energy consumption of 0.470 MW and an operational cost of 0.5891\$/m³ ($C_{E,\ j}$ =0.0336\$/m³, $C_{B,\ j}$ =0.5389\$/m³, $C_{M,\ j}$ =0.0167\$/m³), for a two-stage process ($WR_{sum,\ j}$ =83.39%, $Q_{p,\ sum,\ j}$ =10021 m³/d). From these results, distinct energy output points, for each of which the grid electricity fraction to renewable energy fraction is altered, are defined (0.2 MW, 0.3 MW, 0.4 MW and 0.5 MW).

The Energy Optimization Model is used to determine the minimized cost of an energy supply process with a constant energy output, which is altered between 0.2 MW and 0.5 MW. For each of the energy demand points, the available grid electricity is defined as a fraction of the necessary energy supply and is changed from 0% to 100% in 20% increments. Only solar and wind energy are considered as renewable energy sources.

The results are summarized in Fig. 6, where the energy cost factor in [\$/h] depending on the grid electricity fraction for energy outputs from 0.2 MW to 0.5 MW is shown. As expected, the energy cost factor decreases for an increasing amount of grid electricity fraction. The energy cost factor also decreases for a lower energy output demand for a constant fraction of grid electricity.

To further evaluate the results, the energy cost factor has been transformed with the constant energy output, for each case respectively, to [\$/MWh], see Fig. 7. In this case, the energy output demand for each fraction of grid electricity point does not influence the energy cost factor. Overall, the energy cost factor exhibits an almost linear decline ($R^2 = 0.99$ for the case of 0.2 MW) with an increasing amount of grid electricity. Since the energy costs for varying fractions of grid electricity are approximately the same (maximal deviation of 0.8% in the case of 0% grid electricity between 0.2 MW and 0.4 MW), the determined energy cost factors for 0.2 MW (black line in Fig. 7) have been selected arbitrarily as representative costs to be used in the following design optimization.

It is important to mention that in all cases, storage systems are needed to satisfy the energy demand, except for the case of 100% grid electricity. The cost and the capacity of storage systems are always taken into account for determining the overall energy cost factor of distinct

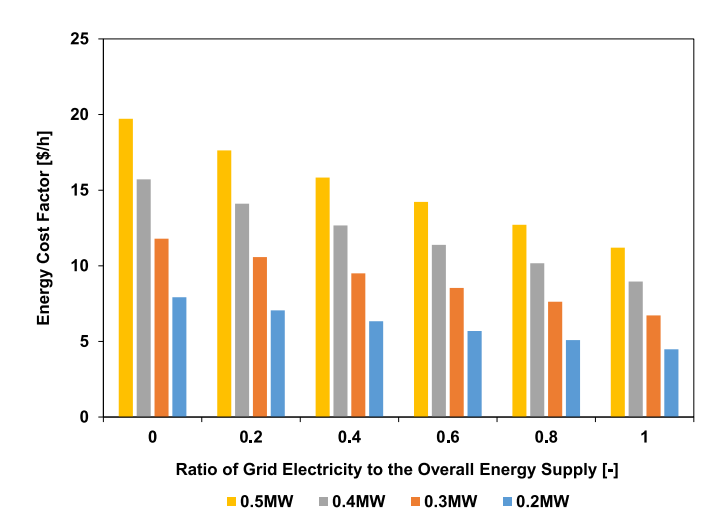


Fig. 6. Energy cost factor e_c in [\$/h] for varying fractions of grid electricity for a constant energy output between 0.2 MW to 0.5 MW.

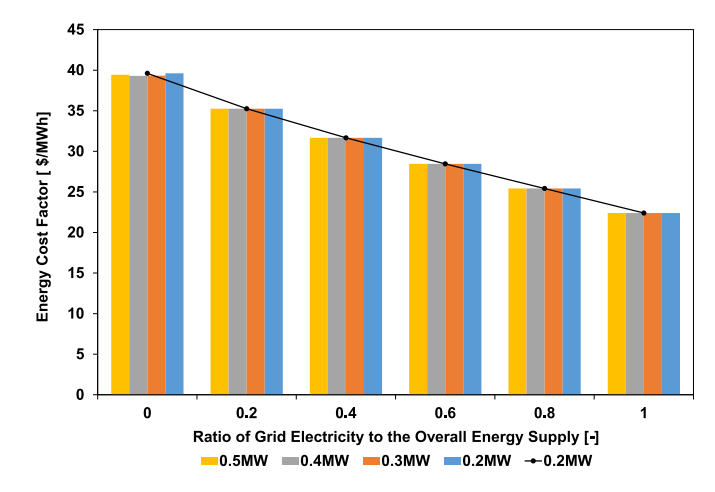


Fig. 7. Energy cost factor e_c in [\$/MWh] for varying fractions of grid electricity for a constant energy output between 0.2 MW to 0.5 MW.

supply scenarios. For all cases, only solar energy is selected because one wind turbine already satisfies much higher energy demands than necessary and is more expensive than the determined necessary amount of solar panels.

Pareto Front for varying energy supply systems, meaning fractions of grid electricity to the overall energy supply, have been created by minimizing the energy cost for changing permeate output flow restrictions ($Q_{p, sum} \ge Q_{p, restriction}$). The results can be found in Fig. 8.

The output permeate flow has been restricted between $Q_{D_{i}}$ restriction=1500 m³/d and 10,000 m³/d. All Pareto Front show the same general behavior: From 1500 m³/d to 3000 m³/d, the energy cost factor increases only marginally (maximum of 12% increase for 0% grid electricity). Then, from 3000 m³/d to 10,000 m³/d, the cost factor increases almost linearly in all cases. For 0% grid electricity, the energy costs are the highest, whereas 100% grid electricity results in the lowest energy cost case. Accordingly, the increment grid electricity supply fractions give energy cost sequences in between 0% and 100% grid electricity supply. An interesting result can be assessed when the two boundary cases of 0% and 100% grid electricity are being compared: the energy cost factor increases by 77% when grid electricity decreases from 100% to 0%. The energy cost, however, rises between 57% (for $Q_{\rm p}$ $sum=1500 \text{ m}^3/\text{d}$) and 80% (for Q_p , $sum=10000 \text{ m}^3/\text{d}$) with the same decrease in grid electricity. So depending on the necessary output permeate flow, a smaller energy cost increase compared to the energy cost factor increase is observed (for $Q_{p, sum} \le 7500 \text{ m}^3/\text{d}$, the energy cost increase is ≤77%). Thus, these indirect savings can be exploited in

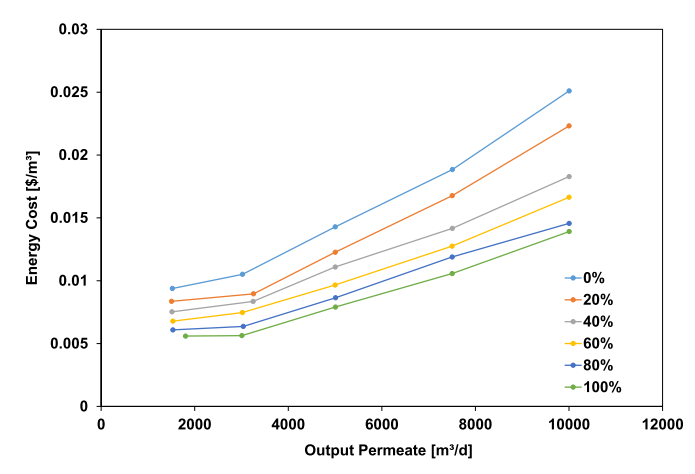


Fig. 8. Results of minimizing energy cost for changing output permeate restrictions and varying grid electricity fractions (from 0% to 100% in 20% increments).

future applications, since the expectation that the energy cost increase is proportional to the energy cost factor increase is negated with the developed optimization model.

To further evaluate the determined optimization results, the energy consumption for each fraction of the grid electricity case has been calculated in $[kWh/m^3]$ and is illustrated depending on the permeate output flow of the system in Fig. 9. Generally, the same behavior as in Fig. 8 can be seen: for a permeate output of $1500 \, \text{m}^3/\text{d}$ to $3000 \, \text{m}^3/\text{d}$, the energy consumption increases only marginally, whereas, the energy consumption increases almost linearly (from $3000 \, \text{m}^3/\text{d}$ to $10,000 \, \text{m}^3/\text{d}$). In this case, however, a clear distinction between the grid electricity fractions is not possible. Therefore, Fig. 11 in Appendix B shows all energy consumption points in $[kWh/m^3]$ depending on the permeate output and independent of the grid electricity fraction. These points can be linearly approximated with a residual of $R^2 = 0.97$ (blue dotted line). Hence, the energy consumption of all systems increases with increasing output permeate water flow, as expected. All determined results of this case study can be found in Appendix B, Table 10.

7.2.2. Scenario II: water for irrigation

For the second scenario, restrictions concerning the available water sources are needed for each water type, respectively. Otherwise, the water source with the lowest total dissolved solids concentration is always chosen (for all here presented objective functions), which is generally surface water. At certain feed flows $(Q_{f,1})$ this is not sustainable anymore since a river or lake is drained empty. Therefore, a realistic representation of flow restrictions is necessary.

To consider a viable restriction for surface water (water from the Medina River in this case), a water treatment facility at Lake Medina, operated by SAWS, was analyzed. When working at full capacity, the plant can treat $13000 \frac{\text{acreft}}{\text{year}}$. Having said this, the plant has not been operated at full capacity since 2013. To ensure a reasonable water level of Lake Medina, one third of the maximum capacity is implemented as a feed flow restriction, $Q_{f, 1, M} \leq 15000 \text{ m}^3/\text{d}$ [76,77]. Derived from the highest possible feed volume flows of the H2Oaks Desalination plant, which uses water from the Carrizo-Wilcox aquifer, a feed flow restriction of $Q_{f, 1, A} \leq 35000 \text{ m}^3/\text{d}$ is defined [64].

Technically, a restriction for a seawater input flow is not required, due to the absence of restrictions concerning seawater discharge flows. However, an arbitrarily chosen limitation of Q_f , 1, 1, 100000 m 3 /d is implemented to maintain applicability of the seawater desalination plant and take into account technical limitations. At certain high volume flows, a second desalination plant would be built rather than trying to further increase the capacity of the original one [64].

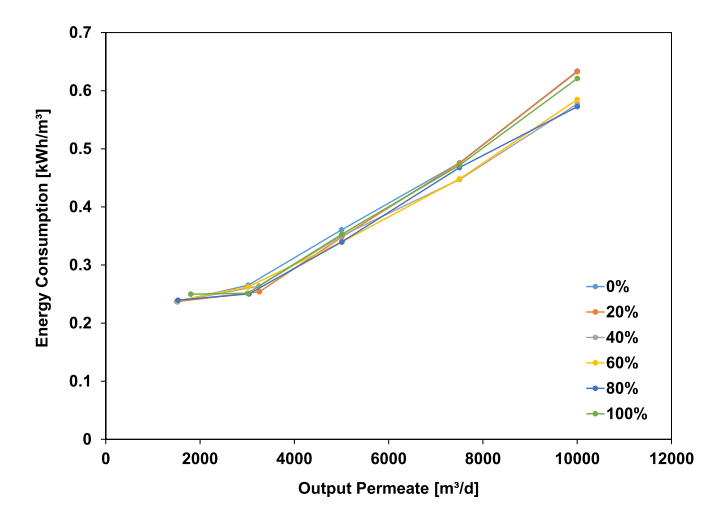


Fig. 9. Energy consumption of an energy cost minimized process with changing output permeate restrictions and varying grid electricity fractions (from 0% to 100% in 20% increments).

To generate a Pareto Front of operational costs and permeate flow, the operational costs are minimized, while the permeate flow restriction $(Q_p, sum, j \ge Q_p, sum, set)$ has been altered from $Q_p, sum, set = 200 \text{ m}^3/\text{d}$ to $60,000 \text{ m}^3/\text{d}$, while three different water sources $j = (Medina \ River \ (M), Carrizo-Wilcox Aquifer (A), Seawater (S)) were considered. The results are summarized in Appendix B, Table 11, as well as in Fig. 10.$

In Fig. 10 the Pareto Front for minimizing operational cost and maximizing the permeate flow for surface water (blue circles), aquifer water (orange circles) and seawater (dark blue circles) can be seen. Optimizing the operational cost while the first permeate flow restriction $(Q_{p, sum, set}=200 \text{ m}^3/\text{d})$ is enforced already results in a permeate flow of $Q_{D, sum, M}$ =6299 m³/d. Consequently, when one is interested in generating a permeate flow between 200 m³/d and 6299 m³/d, a permeate flow of 6299 m³/d results in minimal operational costs, meaning that a higher permeate flow is advantageous here. For other restrictions, the same behavior can be seen, but not as significantly as for the first restriction (see Table 11). A reason for this correlation could be that at a certain volume flow, parallel flows per stage become more advantageous resulting in lower pressures and consequently lower energy costs. Additionally, less membrane surface per stage can be sufficient due to the parallel flow arrangement. This explanation can be compared to the economy of scales, meaning that depending on the desalination process scale, cost advantages can be found.

However, when the feed flow restriction of surface water $(Q_{j, 1, M} \leq 15000 \, \mathrm{m}^3/\mathrm{d})$ is reached, aquifer water is utilized next. With the increase of the feed total dissolved solids concentration, an operational cost level jump from around $0.0187\$/\mathrm{m}^3$ to $0.0431\$/\mathrm{m}^3$ can be seen. For surface and aquifer water, respectively, the price for increasing the permeate flow over the whole possible range rises moderately (surface water: 9.5%, aquifer water: 3.3%). However, the operational cost more than doubles when the water source is switched from surface to aquifer water.

The same effect can be seen when the water source is specified as seawater instead of a quifer water (due to the feed flow restriction $Q_{f,\,1,\,A} \leq 35000~{\rm m}^3/{\rm d}$): the operational cost increases from around 0.0431 \$\frac{9}{m}\$ to 4.4502\$/m\$^3. When seawater operational costs are compared to the operational costs of the other two water sources, one can see that a quifer and surface water operational costs are negligible in regard to seawater processes.

Overall, it can be seen how much more cost intensive seawater desalination is. On the other hand, significantly higher permeate flows are possible. For certain water demand scenarios (here $Q_{p, sum, j} \geq 35000$ m³/d), seawater is the only water source which can satisfy the given demand without substantial environmental impacts (e.g. by draining an aquifer or river linked with unforeseeable consequences for ecosystems). Moreover, with the Pareto Front in Fig. 10, the tradeoff between reducing operational costs for as high as possible water outputs has

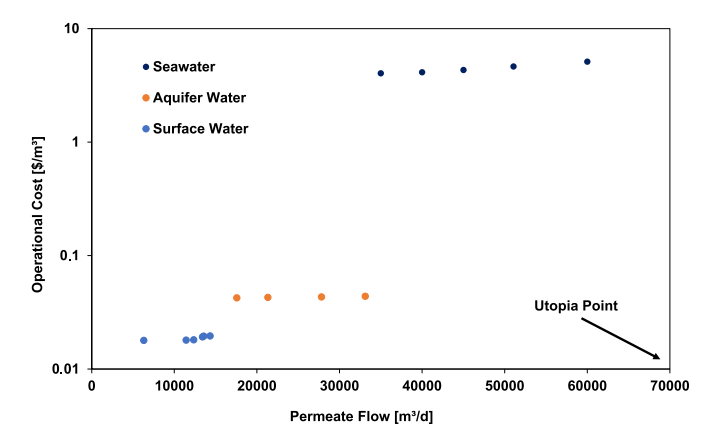


Fig. 10. Pareto front for minimizing operational costs for varying permeate flow restriction (lower bound), for surface water, aquifer water and seawater. (For interpretation of the references to color in this figure, the reader is referred to the web version of this article.)

Table 2 Overview results design optimization minimizing operational costs with seawater and grid electricity ($Q_{f, 1} \le 100000 \text{ m}^3/\text{d}$, $C_{f, 1} = 34000 \text{ mg/L}$, $Q_{p, sum} \ge 35000 \text{ m}^3/\text{d}$).

Stage	Q_f [m ³ /d]	C_f [mg/L]	P [bar]	WR [%]	A [m ²]	C_p [mg/L]	C_r [mg/L]	$m_{i,j}$
Stage 1	59,276	34,000	41.82	64.92	3626	5273	87,150	5
Stage 2	38,479	5273	5.015	69.88	351	3236	10,000	1
Stage 3	11,590	10,000	5.002	69.99	120	60	33,178	1

successfully been visualized.

7.2.3. Scenario III: water for power generation

The focus of the third case study is to evaluate the impact of changing energy sources on the design of seawater desalination plants producing water for cooling purposes in power generation plants. To determine a representative daily water demand of a power plant, a typical Texan power generation facility is selected. Since Texas' primary energy source is natural gas [78], the Sim Gideon Natural Gas Power Plant in Bastrop, Texas (South-Central Texas) is chosen. The plant is taking its cooling water from Lake Bastrop [79], which is a freshwater reservoir, so a closed-loop reservoir cooling system is assumed, which demands approximately 2200 L/MWh water [80]. Because of the plant's maximum capacity of 620 MW [79], the highest possible daily water demand is $32,736 \, \text{m}^3/\text{d}$. To be on the safe side, a permeate output restriction of $Q_{D. Sum} \geq 35000 \, \text{m}^3/\text{d}$ is enforced.

Now, the minimal operational cost plant design, depending on the energy supply system (energy supply only by grid electricity or only by solar and wind energy), for satisfying at least a permeate flow of Q_p , $sum \ge 35000 \text{ m}^3/\text{d}$ can be determined. Results of the design optimization when only grid electricity (e_c =22.4\$/MWh) is used as an energy source can be found in Tables 2 and 3.

For minimizing operational costs, a three-stage process is suggested with an overall water recovery of WR_{sum, grid}=59%. For a seawater desalination process, the calculated water recovery is comparably high, underlining that high water recoveries result in lower brine disposal costs. The process results in an operational power generation cooling water process cost of $13.011 \frac{\$}{10^3 \cdot gal}$. These obtained operational costs are comparably high for a seawater process (usually 10 to 12 $\frac{\$}{10^3 \cdot gal}$, taken from the Texas Desalination 2019 Conference). Looking at the energy consumption of 2.3482 kWh/m³ for the process, it can be seen that in terms of energy consumption the process is very competitive [35]. The energy cost of a seawater RO desalination process is specified in [24] to be 0.311\$/m3. The here elaborated energy cost is 0.0526\$/m3, so approximately six times cheaper. Focusing on the composition of the operational costs shows that the major cost driver is the brine disposal cost. However, the challenges arising for seawater reverse osmosis are the construction of seawater intakes and concentrated brine ocean discharge systems, which are considered as capital costs constituents, rather than the disposal itself [81,82]. Consequently, it can be derived that the used brine concentration disposal cost function results in comparably high values for seawater desalination processes.

Next, a design optimization for minimizing the operational costs of a seawater desalination process only using solar and wind energy is performed. Therefore, the energy optimization model is used to generate an energy cost function for solar and wind energy under consideration of energy storage systems. The result of this optimization can be seen in Fig. 12 in Appendix B. The slope of the shown nearly linear ($R^2 = 0.996$) relationship between total cost (investment and operational costs) of the energy supply system in [\$/h] and the desired power output in [MW] is

 e_c =29.84\$/MWh. Now, with the specified renewable energy consumption cost, design optimization can be performed. The generated results for the design optimization of a desalination process only using renewable energies for minimizing operational costs can be seen in Tables 4 and 5.

The results are comparable to the ones obtained by the design optimization with grid electricity. The energy cost factor increases from grid electricity to renewable energies by 33%. Accordingly, the energy cost increases as well by 33%, but the operational costs are approximately constant (an increase of 0.12%). In contrast, Di Martino et al. found cost savings in this case for brackish water desalination processes producing drinking water, meaning that with an increasing energy cost factor of 33% the operational cost only increases by 11% [83]. Thus, these principles are not applicable for seawater desalination systems. In the here presented case, the energy source has virtually no effect on the operational costs due to the high brine disposal costs. In subsequent work, sensitivity analyses concerning the impact of the electricity cost on the operational cost for increasing electricity prices should be performed to evaluate if an electricity price influence boundary exists. This concludes the presented case studies for the design optimization model, showing the versatility of the developed framework for desalination processes, as well as the potential for saving energy and operational costs for reverse osmosis systems in general.

8. Conclusion

The goal of this work is to develop a framework methodology that incorporates various input energy and input water sources to satisfy increasing water demands for regions that are characterized by water scarcity (e.g. South Central Texas). Consequently, depending on the available input resources, the membrane system as well as the operating parameters of the desalination system change. The approach presented here can be modified for distinct regions and incorporate the given limitations or availabilities of water or energy sources. Additionally, the water quality output of the reverse osmosis process can be adjusted to the desired water application, so that not only municipal water usage can be considered, but also applications like irrigation or livestock. A superstructure representation and optimization are then used as part of the developed framework to generate optimal desalination designs. Thus, a plethora of optimal solutions for scenario analyses can be created. The incorporated approach enables a systematic process systems engineering approach for reverse osmosis desalination process possibilities dependent on regional factors. Thus, a holistic framework for reverse osmosis desalination, to satisfy an array of partially competing output goals, has been developed.

In three different case studies, each tackling a distinct facet of the food-energy-water nexus, the applicability of the framework has been illustrated. By changing the fraction of grid electricity of the energy supply system of a desalination plant producing drinking water, an environmental metric can indirectly be incorporated. Additionally, a linear approximation of the energy consumption of the system independently of the grid electricity fraction could be determined. Moreover,

Table 3 Operational costs design optimization minimizing operational costs with seawater and grid electricity ($Q_{f,1} \le 100000 \,\mathrm{m}^3/\mathrm{d}$, $C_{f,1} = 34000 \,\mathrm{mg/L}$, $Q_{p,sum} \ge 35000 \,\mathrm{m}^3/\mathrm{d}$).

Energy costs	Brine costs	Membrane costs	Total operational costs	Total operational costs
[\$/m ³]	[\$/m ³]	[\$/m ³]	[\$/m ³]	[\$/1000 gal]
0.0526	3.366	0.0054	3.424	13.011

Table 4 Overview results design optimization minimizing operational costs with seawater and renewable energies (only solar and wind, $Q_{f,1} \le 100000 \text{ m}^3/\text{d}$, $C_{f,1} = 34000 \text{ mg/d}$ L, $Q_{p, sum} \ge 35000 \,\mathrm{m}^3/\mathrm{d}$).

Stage	Q_f [m ³ /d]	C_f [mg/L]	P [bar]	WR [%]	A [m ²]	C_p [mg/L]	C_r [mg/L]	$m_{i,j}$
Stage 1	59,182	34,000	41.53	65.39	3690	5429	87,968	5
Stage 2	38,696	5429	5.022	68.18	299	3297	10,000	1
Stage 3	12,312	10,000	5.001	69.98	113	60	33,170	1

Table 5 Operational costs design optimization minimizing operational costs with seawater and renewable energies (only solar and wind, $Q_{f,1} \le 100000 \text{ m}^3/\text{d}$, $C_{f,1} = 34000 \text{ mg/d}$) L, $Q_{p, sum} \ge 35000 \text{ m}^3/\text{d}$).

Energy costs	Brine costs	Membrane costs	Total operational costs	Total operational costs
[\$/m ³]	[\$/m ³]	[\$/m ³]	[\$/m ³]	[\$/1000 gal]
0.0699	3.353	0.0055	3.428	13.026

a Pareto Front for minimizing operational cost and maximizing the permeate flow for water for irrigation was visualized. For water for power generation applications with seawater as a water source, the influence of changing energy supply systems on the desalination plant design has been evaluated.

To summarize, the key contributions of this work are:

- 1. A reliable and fast screening of reverse osmosis plant designs prior to detailed plant modeling.
- 2. The development of a techno-economic and feasibility analysis of desalination plants.
- 3. The enabling and facilitating of various possible scenario analyses.
- 4. The implementation of a Water-Energy Nexus approach, in an attempt to tackle water scarcity challenges for arid and semi-arid regions, considering not only the modeling and optimization of desalination systems but also the energy supply system of the process.

Future works can entail modifications of the framework methodology to increase model accuracy and applicability. For example, other desalination process steps can be included additionally in the framework approach, like pre- and posttreatment. Also, recycle streams or bypasses can be incorporated. Generally, this framework can be expanded and applied to other desalination technologies and hybrid desalination process designs, with the aim of developing a tool to adequately rate desalination alternatives. Moreover, investment costs as well as membrane cleaning costs and other cost factors can be added in future works.

CRediT authorship contribution statement

Marcello Di Martino: Methodology, Software, Formal analysis, Investigation, Writing - Original Draft, Visualization.

Styliani Avraamidou: Conceptualization, Validation, Writing - Review & Editing, Supervision.

Julie Cook: Methodology, Software, Investigation, Writing - Review & Editing.

Efstratios N. Pistikopoulos: Conceptualization, Resources, Writing - Review & Editing, Supervision, Funding acquisition.

Nomenclature

List of abbreviations

DOF	Degrees of Freedom
ERD	Energy Recovery Device
MILP	Mixed-Integer Linear Pro

ogramming **MINLP** Mixed-Integer Nonlinear Programming

MIP Mixed-Integer Programming NLP Nonlinear Programming PSE **Process Systems Engineering**

RO Reverse Osmosis

SARA San Antonio River Authority SAWS San Antonio Water System TDSTotal Dissolved Solids

TWDB Texas Water Development Board

Index directory

В Brine Cost

demand Set Demand Restriction

Ε Energy f Feed Stream i Stage i j Water Source j М Membrane

Necessary operational value nec

Permeate Stream

ритр Input Value for Pumping Operation

Retentate Stream Residual Variable res restriction Set Quality Restriction Dissolved Salts

sum Summation of Variables Membrane Pressure Vessel

Water

Symbol directory

Efficiency, [-]η

Brine Disposal Cost Function Factor, $\left[\frac{\$}{m^3}\right]$ b_c

Energy Cost Function Factor, $\left[\frac{\$}{m^3}\right]$

 e_c Surface Area, $[m^2]$ Α C Concentration, $\left[\frac{mg}{T}\right]$

J Flux, $\left[\frac{m}{c}\right]$

LS Membrane Lifespan, [years]

Parallel Flows per Stage, [-] m

Membrane Cost, [\$] me

N Number of, [-]Р Pressure, [bar]

Q Volume Flow, $\left[\frac{m^3}{s}\right]$ R Fraction Remainder, [-]

SEC Specific Energy Consumption, $\left[\frac{J}{m^3}\right]$

Membrane Pressure Vessel Cost, [\$]

 $WR = \frac{Q_p}{Q_e}$ Water Recovery, [-]

Declaration of competing interest

The authors declare that they have no known competing financial interests or personal relationships that could have appeared to influence the work reported in this paper.

Acknowledgements

The authors gratefully acknowledge financial support from the Na-

tional Science Foundation under Grant Addressing Decision Support for Water Stressed FEW Nexus Decisions [1739977], and Texas A&M Energy Institute.

Additionally, the authors would like to thank Alexander Mitsos, Moritz Begall and Artur Schweidtmann of the Process Systems Engineering group of the Department of Chemical Engineering of RWTH Aachen University for their feedback and constructive criticism.

Appendix A

Table 6Overview input data for membrane data generation with WAVE. Additional information can be found in the supplementary file.

Feed water	Selected membrane	C_f [mg/L]
Seawater	SW30HRLE-400i	36,000
Brackish water	BW30-400/34	32,000 10,000
		3000
		1500
Surface water	XLE-440	700

Table 7Summary of specifications of used DOW FILMTEC membranes.

Specification	SW30HRLE – 400i	BW30 - 400/34	<i>XLE</i> – 440
Description	Lower lifecycle cost for medium and high salinity feedwaters	High rejection, high surface area	Extra low energy, high productivity
Membrane type	Polyamide thin-film composite	Polyamide thin-film composite	Polyamide thin-film composite
Active area [m ²]	41	37	41
Stabilized salt rejection [%]	99.80	99.50	99.00
Max. pressure [bar]	83	41	41
Max. temperature [K]	318.15	318.15	318.15
pH range	2–11	2–11	2–11
Maximum feed silt density index	SDI 5	SDI 5	SDI 5
Maximum feed silt density index	SDI 5	SDI 5	SDI 5

For additional information please refer to:

https://www.lenntech.com/Data-sheets/Dow-Filmtec-BW30-400.pdf, https://www.lenntech.com/Data-sheets/Dow-Filmtec-BW30-400.pdf, https://www.lenntech.com/Data-sheets/Dow-Filmtec-XLE-440.pdf.

The pressure vessel unit costs in Table 8 are defined for 7 membranes per vessel. The pressure vessel costs reduce to \$800 or \$700, respectively, when a pressure vessel for only one membrane is needed [67].

An overview of the various process input water specifications is given in Table 9. For the total dissolved solids concentration of the Gulf of Mexico, a near coastal drain was assumed. Additionally, all industrial wastewater streams are effluents from industries in San Antonio. Further, the TDS concentration of 700 mg/L for Medina River was measured at the San Antonio River Authority (SARA) station 14195 at Leon Creek, which is a tributary of Medina River. The specification of the salinity of the Carrizo-Wilcox aquifer water was supplied by the H2Oaks Desalination facility and also confirmed by the TWDB.

Table 8
Costs of membrane modules and pressure vessel units (obtained from Consolidated Water Co. Ltd.) [67].

Membrane type	Module cost [\$]	Pressure vessel	Unit cost [\$]	$R_{v,j}$ correlation [\$]
SW30HRLE-400i	695	High pressure	2000	$R_{\nu,j} \cdot \frac{2000 - 800}{7 \cdot 1} + 600$
BW30-400/34	525	Low pressure	1900	$R_{v,j} \cdot \frac{1900 - 700}{7 - 1} + 500$
XLE-440	560	Low pressure	1900	$R_{\nu j} \cdot \frac{1900 - 700}{7 - 1} + 500$

Table 9Desalination input water characterization and definition.

Water type	Water specification	TDS concentration [mg/L]	Source
Seawater	Gulf of Mexico	34,000	[84]
Ground water	Carrizo-Wilcox Aquifer	1500	[64,85]
Surface water	Medina River	700	[86]
Industrial wastewater	Metal Finishing Industry	3000	[87]
	Semi-Conductor Manufacturer	5600	[87]
	Johnson Controls Battery	7600	[87]

Appendix B

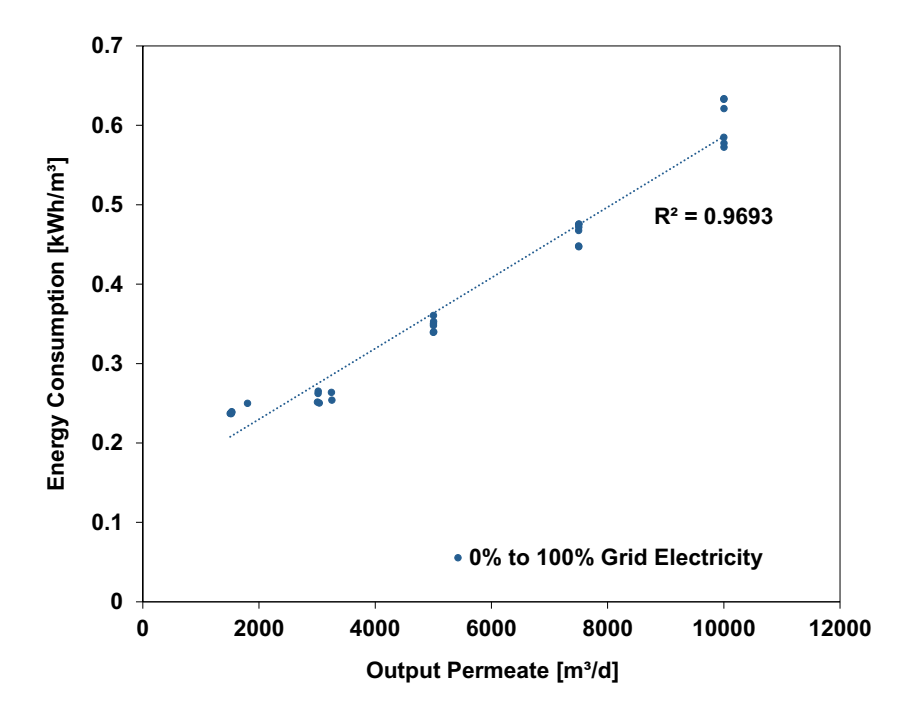


Fig. 11. Linear approximation of the energy consumption of an energy cost minimized process with changing output permeate restrictions and varying grid electricity fractions (from 0% to 100% in 20% increments).

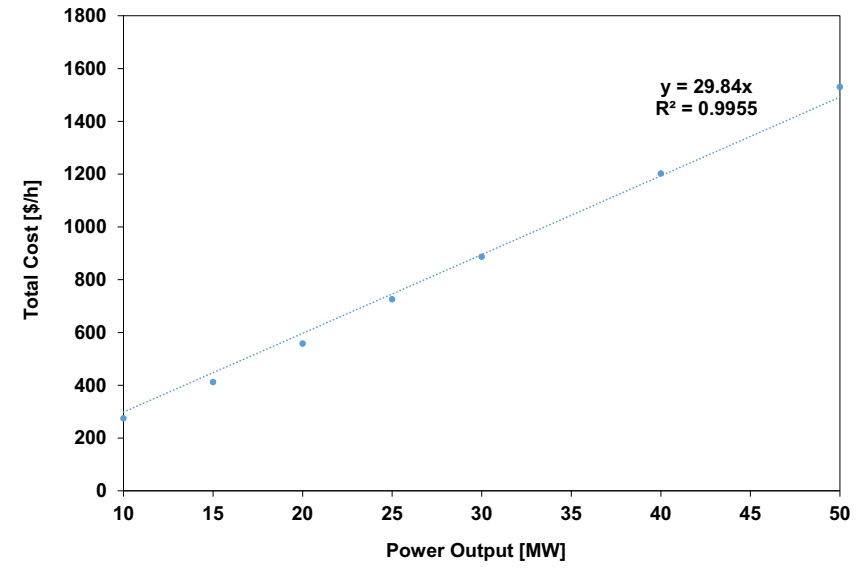


Fig. 12. Energy cost function for renewable energies only using solar and wind (including energy storage).

Table 10 Overview energy cost and energy consumption for varying grid electricity fractions of the energy supply system (grid electricity and renewable energies, FracGrid) for minimizing the energy costs of the system (C_f =5600 mg/L, $Q_f \le 12500$ m³/d, Q_p , $sum \ge Q_p$, restriction).

FracGrid	Energy cost factor	$Q_{p,restriction}$	$Q_{p,sum}$	WR_{sum}	Energy cost	Energy consumption
[-]	[S/MWh]	[m ³ /d]	$[m^3/d]$	[%]	[\$/m ³]	[kWh/m ³]
0.00	39.612	1500	1522	70.00	0.0094	0.237
		3000	3020	84.03	0.0105	0.265
		5000	5003	83.71	0.0143	0.361
		7500	7507	80.04	0.0188	0.476
		10,000	10,002	83.18	0.0251	0.634
0.20	35.261	1500	1504	69.82	0.0084	0.237
		3000	3256	83.55	0.0090	0.254
		5000	5003	83.54	0.0123	0.348
		7500	7502	83.21	0.0168	0.475
		10,000	10,533	83.35	0.0223	0.633
0.40	31.670	1500	1512	69.96	0.0075	0.238
		3000	3247	83.91	0.0084	0.264
		5000	5002	83.72	0.0111	0.350
		7500	7504	83.55	0.0142	0.447
		10,000	10,002	83.47	0.0183	0.577
0.60	28.454	1500	1532	69.51	0.0068	0.238
		3000	3018	83.98	0.0075	0.262
		5000	5001	83.62	0.0097	0.339
		7500	7501	79.52	0.0127	0.448
		10,000	10,000	82.40	0.0166	0.585
0.80	25.427	1500	1532	69.99	0.0061	0.239
		3000	3037	70.37	0.0064	0.250
		5000	5008	83.09	0.0086	0.340
		7500	7502	83.65	0.0119	0.468
		10,000	10,002	82.42	0.0146	0.573
0.00	22.400	1500	1803	84.14	0.0056	0.250
		3000	3008	83.85	0.0056	0.251
		5000	5007	83.71	0.0079	0.353
		7500	7503	82.96	0.0106	0.472
		10,000	10,002	82.44	0.0139	0.621

Table 11
Summary results design optimization case 2, Pareto front (minimizing operational costs vs. maximizing permeate output).

$Q_{p,sum,set}$ [m ³ /d]	$Q_{p,sum}$ [m ³ /d]	Operational cost [\$/m³]	C_f [mg/L]
200	6299	0.0179	700
6500	11,431	0.0180	700
12,000	12,348	0.0181	700
13,000	13,416	0.0192	700
13,500	13,561	0.0195	700
14,000	14,329	0.0196	700
15,000	17,565	0.0424	1500
18,000	21,329	0.0428	1500
22,000	27,823	0.0432	1500
32,000	33,114	0.0438	1500
35,000	35,000	4.0442	34,000
40,000	40,003	4.1243	34,000
45,000	45,005	4.3222	34,000
50,000	51,064	4.6393	34,000
60,000	60,000	5.1208	34,000

Appendix C. Supplementary data

Supplementary data to this article can be found online at https://doi.org/10.1016/j.desal.2021.114937. The supplementary file summarizes and specifies the reverse osmosis model development, the energy optimization model, representative operation optimization results, as well as performed sensitivity analyses.

References

- Jorge Arroyo, Sanjeev Kalaswad, Water desalination in Texas, TWDB, 2015, URL: https://www.twdb.texas.gov/innovativewater/desal/doc/DesalTexasUSWate rNews.pdf.
- [2] Margaret Wilder, Ismael Aguilar-Barajas, Nicolás Pineda Pablos, Robert Varady, Desalination and water security in the US-Mexico border region: assessing the social, environmental and political impacts, Water Int. 41 (2016) 756–775, https://doi.org/10.1080/02508060.2016.1166416.
- [3] Khawla Abdul Mohsen Al-Shayji, Modeling, Simulation and Optimization of largescale Commercial Desalination Plants (Dissertation), Virginia Polytechnic Institute and State University, Blacksburg, Virginia, USA, 1998. URL: http://hdl.handle. net/10919/30462.
- [4] Daniel J. Garcia, Fengqi You, The water-energy-food nexus and process systems engineering: a new focus, Compu. Chem. Eng. 91 (2016) 49–67, https://doi.org/ 10.1016/j.compchemeng.2016.03.003.
- [5] Negar Vakilifard, Parisa A. Bahri, Martin Anda, Goen Ho, An interactive planning model for sustainable urban water and energy supply, Appl. Energy 235 (2019) 332–345, https://doi.org/10.1016/j.apenergy.2018.10.128.

- [6] R. Cory Allen, Yaling Nie, Styliani Avraamidou, Efstratios N. Pistikopoulos, Infrastructure planning and operational scheduling for power generating systems: an energy-water nexus approach, Comput. Aided Chem. Eng. 47 (2019) 233–238, https://doi.org/10.1016/B978-0-12-818597-1.50037-0.
- [7] Yaling Nie, Styliani Avraamidou, Xin Xiao, Efstratios N. Pistikopoulos, Jie Li, Yujiao Zeng, Fei Song, Jie Yu, Min Zhu, A food-energy-water nexus approach for land use optimization, Sci. Total Environ. 659 (2019) 7–19, https://doi.org/ 10.1016/j.scitotenv.2018.12.242.
- [8] R. Cory Allen, Yaling Nie, Styliani Avraamidou, Efstratios N. Pistikopoulos, Xin Xiao, A multi-objective energy-water nexus planning model: a case study of the power systems in Texas Edwards aquifer, URL: https://aiche.confex.com/aich e/2018/meetingapp.cgi/Paper/534130, 2018.
- [9] Styliani Avraamidou, Stefanos G. Baratsas, Yuhe Tian, Efstratios N. Pistikopoulos, Circular economy - a challenge and an opportunity for process systems engineering, Comput. Chem. Eng. 133 (2020) 106629, https://doi.org/10.1016/j. compchemeng.2019.106629.
- [10] Roberta Fornarelli, Parisa A. Bahri, Martin Anda, Goen Ho, Farhad Shahnia, Ali Arefi, The energy-water nexus: renewable energy and water desalination, in: 15th World Renewable Energy Congress, 2016. URL: https://researchrepository.murdoch.edu.au/id/eprint/40223/.
- [11] Ximing Cai, Kevin Wallington, Majid Shafiee-Jood, Landon Marston, Understanding and managing the food-energy-water nexus – opportunities for water resources research, Adv. Water Resour. 111 (2018) 259–273, https://doi. org/10.1016/j.advwatres.2017.11.014.
- [12] Ilhan Ozturk, Sustainability in the food-energy-water nexus: evidence from brics (Brazil, the Russian Federation, India, China, and South Africa) countries, Energy 93 (2015) 999–1010, https://doi.org/10.1016/j.energy.2015.09.104.
- [13] Kelly M. Kibler, Debra Reinhart, Christopher Hawkins, Amir Mohaghegh Motlagh, James Wright, Food waste and the food-energy-water nexus: a review of food waste management alternatives, Waste Manag. (New York N.Y.) 74 (2018) 52–62, https://doi.org/10.1016/j.wasman.2018.01.014.
- [14] Xin Guan, Giuseppe Mascaro, David Sampson, Ross Maciejewski, A metropolitan scale water management analysis of the food-energy-water nexus, Sci. Total Environ. 701 (2020) 134478, https://doi.org/10.1016/j.scitotenv.2019.134478.
- [15] Stacia J. Dreyer, Tim Kurz, Annayah M.B. Prosser, Abigail Abrash Walton, Kelley Dennings, Ilona McNeill, Deborah A. Saber, Janet K. Swim, Towards a psychology of the food–energy–water nexus: costs and opportunities, J. Soc. Issues 76 (2020) 136–149. https://doi.org/10.1111/josi.12361.
- [16] Bridget R. Scanlon, Ben L. Ruddell, Patrick M. Reed, Ruth I. Hook, Chunmiao Zheng, Vince C. Tidwell, Stefan Siebert, The food-energy-water nexus: transforming science for society, Water Resour. Res. 53 (2017) 3550–3556, https://doi.org/10.1002/2017WR020889.
- [17] P. Abdul Salam, Sangam Shrestha, Vishnu Prasad Pandey, Anil Kumar Anal (Eds.), Water-energy-food Nexus: Principles and Practices, AGU, Hoboken, NJ, 2017 volume 229 of Geophysical monograph series. URL: http://onlinelibrary.wiley.com/pook/10.1002/9781119243175.
- [18] Somayeh Asadi, Behnam Mohammadi-Ivatloo, Food-energy-water Nexus Resilience and Sustainable Development: Decision-making Methods, Planning, and Trade-off Analysis, 1st ed., 2020, https://doi.org/10.1007/978-3-030-40052-1, 2020 ed
- [19] Satinder Ahuja (Ed.), Food, Energy, and Water, Elsevier, Amsterdam, 2015. URL: https://www.elsevier.com/books/food-energy-and-water/ahuja/978-0-12-8002
- [20] P. Saundry, B.L. Ruddell, The Food-energy-water Nexus, in: AESS Interdisciplinary Environmental Studies and Sciences Series, 2020, https://doi.org/10.1007/978-3-030-29914-9, 2020 ed., URL:.
- [21] Yoshihide Wada, Ludovicus P.H. van Beek, Cheryl M. van Kempen, Josef W.T. M. Reckman, Slavek Vasak, Marc F.P. Bierkens, Global depletion of groundwater resources, Geophys. Res. Lett. 37 (2010), https://doi.org/10.1029/ 2010G1044571
- [22] Robin Kundis Craig, Water supply, desalination, climate change, and energy policy symposium: critical intersections for energy & water law: exploring new challenges and opportunities, Pac. McGeorge Glob. Bus. Develop. Law J. 2 (2010) 225–255.
- [23] Mutiara Ayu Sari, Shankararaman Chellam, Reverse osmosis fouling during pilot-scale municipal water reuse: evidence for aluminum coagulant carryover, J. Membr. Sci. 520 (2016) 231–239, https://doi.org/10.1016/j. memsci 2016 07 029
- [24] Lauren F. Greenlee, Desmond F. Lawler, Benny D. Freeman, Benoit Marrot, Philippe Moulin, Reverse osmosis desalination: water sources, technology, and today's challenges, Water Res. (2009) 2317–2348, https://doi.org/10.1016/j. watres.2009.03.010.
- [25] Georgios Patroklou, Iqbal M. Mujtaba, Economic optimisation of seawater reverse osmosis desalination with boron rejection, Comput. Aided Chem. Eng. 33 (2014) 1381–1386, https://doi.org/10.1016/B978-0-444-63455-9.50065-9.
- [26] Larry X. Gao, Han Gu, Anditya Rahardianto, Panagiotis D. Christofides, Yoram Cohen, Self-adaptive cycle-to-cycle control of in-line coagulant dosing in ultrafiltration for pre-treatment of reverse osmosis feed water, Desalination 401 (2017) 22–31, https://doi.org/10.1016/j.desal.2016.09.024.
- [27] Muhammad Qasim, Mohamed Badrelzaman, Noora N. Darwish, Naif A. Darwish, Nidal Hilal, Reverse osmosis desalination: a state-of-the-art review, Desalination (2019) 59–104, https://doi.org/10.1016/j.desal.2019.02.008.
- [28] Kah Peng Lee, Tom C. Arnot, Davide Mattia, A review of reverse osmosis membrane materials for desalination - development to date and future potential, J. Membr. Sci. (2011) 1–22, https://doi.org/10.1016/j.memsci.2010.12.036.

- [29] Jad R. Ziolkowska, Reuben Reyes, Prospects for desalination in the united states experiences from california, florida and texas, in: Competition for Water Resources, 2017, pp. 298–316, https://doi.org/10.1016/B978-0-12-803237-4.00017-3.
- [30] Ignacio E. Grossmann, Gonzalo Guillén-Gosálbez, Scope for the application of mathematical programming techniques in the synthesis and planning of sustainable processes, Comput. Chem. Eng. 34 (2010) 1365–1376, https://doi.org/ 10.1016/j.compchemeng.2009.11.012.
- [31] Gonzalo Guillen-Gosalbez, Fengqi You, Angel Galan-Martin, Carlos Pozo, Ignacio E. Grossmann, Process systems engineering thinking and tools applied to sustainability problems: current landscape and future opportunities, Curr. Opin. Chem. Eng. 26 (2019) 170–179, https://doi.org/10.1016/j.coche.2019.11.002.
- [32] Luca Mencarelli, Qi Chen, Alexandre Pagot, Ignacio E. Grossmann, A review on superstructure optimization approaches in process system engineering, Comput. Chem. Eng. 136 (2020) 106808, https://doi.org/10.1016/j. compchemeng.2020.106808.
- [33] South Central Texas Regional Water Planning Group, TWDB, 2016 South-Central Texas Regional Water Plan: Volume I - Executive Summary and Regional Water Plan, URL: https://www.twdb.texas.gov/waterplanning/rwp/plans/2016/L/Regi on L 2016 RWPV1.ndf, 2015.
- [34] Daniel J. Garcia, Brittainy M. Lovett, Fengqi You, Considering agricultural wastes and ecosystem services in food-energy-water-waste nexus system design, J. Clean. Prod. 228 (2019) 941–955, https://doi.org/10.1016/j.jclepro.2019.04.314.
- [35] Amin Ghobeity, Alexander Mitsos, Optimal design and operation of desalination systems: new challenges and recent advances, Curr. Opin. Chem. Eng. (2014) 61–68, https://doi.org/10.1016/j.coche.2014.09.008.
- [36] H. Kotb, E.H. Amer, K.A. Ibrahim, On the optimization of RO (reverse osmosis) system arrangements and their operating conditions, Energy 103 (2016) 127–150, https://doi.org/10.1016/j.energy.2016.02.162.
- [37] M.A. Al-Obaidi, C. Kara-Zaïtri, Iqbal M. Mujtaba, Performance evaluation of multistage reverse osmosis process with permeate and retentate recycling strategy for the removal of chlorophenol from wastewater, Comput. Chem. Eng. 121 (2019) 12–26, https://doi.org/10.1016/j.compchemeng.2018.08.035.
- [38] Amin Ghobeity, Alexander Mitsos, Optimal time-dependent operation of seawater reverse osmosis, Desalination 263 (2010) 76–88, https://doi.org/10.1016/j. desal.2010.06.041.
- [39] Aihua Zhu, Panagiotis D. Christofides, Yoram Cohen, Effect of thermodynamic restriction on energy cost optimization of ro membrane water desalination, Ind. Eng. Chem. Res. 48 (2009) 6010–6021, https://doi.org/10.1021/ie800735q.
- [40] Mojibul Sajjad, Mohammad G. Rasul, Simulation and optimization of solar desalination plant using Aspen Plus simulation software, Proc. Eng. (2015) 739–750, https://doi.org/10.1016/j.proeng.2015.05.065.
 [41] Amin Ghobeity, Corey J. Noone, Costas N. Papanicolas, Alexander Mitsos, Optimal
- [41] Amin Ghobeity, Corey J. Noone, Costas N. Papanicolas, Alexander Mitsos, Optimal time-invariant operation of a power and water cogeneration solar-thermal plant, Sol. Energy 85 (2011) 2295–2320, https://doi.org/10.1016/j. solener.2011.06.023.
- [42] Somayyeh Sadri, Mohammad Ameri, Ramin Haghighi Khoshkhoo, Multi-objective optimization of med-tvc-ro hybrid desalination system based on the irreversibility concept, Desalination 402 (2017) 97–108, https://doi.org/10.1016/j. desal.2016.09.029.
- [43] O.M.A. Al-hotmani, M.A. Al-Obaidi, R. Patel, Iqbal M. Mujtaba, Performance analysis of a hybrid system of multi effect distillation and permeate reprocessing reverse osmosis processes for seawater desalination, Desalination 470 (2019) 114066, https://doi.org/10.1016/j.desal.2019.07.006.
- [44] Yousef Saif, Ali Elkamel, Mark Pritzker, Global optimization of reverse osmosis network for wastewater treatment and minimization, Ind. Eng. Chem. Res. 47 (2008) 3060–3070, https://doi.org/10.1021/ie071316j.
- [45] Du Yawei, Lixin Xie, Yuxin Wang, Yingjun Xu, Shichang Wang, Optimization of reverse osmosis networks with spiral-wound modules, Ind. Eng. Chem. Res. 51 (2012) 11764–11777, https://doi.org/10.1021/ie300650b.
- [46] Du Yawei, Lixin Xie, Jie Liu, Yuxin Wang, Yingjun Xu, Shichang Wang, Multiobjective optimization of reverse osmosis networks by lexicographic optimization and augmented epsilon constraint method, Desalination 333 (2014) 66–81, https://doi.org/10.1016/j.desal.2013.10.028.
- [47] Cheng Seong Khor, Dominic C.Y. Foo, Mahmoud M. El-Halwagi, Raymond R. Tan, Nilay Shah, A superstructure optimization approach for membrane separationbased water regeneration network synthesis with detailed nonlinear mechanistic reverse osmosis model, Ind. Eng. Chem. Res. 50 (2011) 13444–13456, https://doi. org/10.1021/ie200665g.
- [48] Kamal M. Sassi, Iqbal M. Mujtaba, MINLP based superstructure optimization for boron removal during desalination by reverse osmosis, J. Membr. Sci. 440 (2013) 29–39, https://doi.org/10.1016/j.memsci.2013.03.012.
- [49] Kerron J. Gabriel, Mahmoud M. El-Halwagi, Patrick Linke, Optimization across the water–energy nexus for integrating heat, power, and water for industrial processes, coupled with hybrid thermal-membrane desalination, Ind. Eng. Chem. Res. 55 (2016) 3442–3466, https://doi.org/10.1021/acs.iecr.5b03333.
- [50] Mingheng Li, Optimization of multi-stage hybrid ro-pro membrane processes at the water-energy nexus, Chem. Eng. Res. Des. 137 (2018) 1–9, https://doi.org/ 10.1016/j.cherd.2018.06.042.
- [51] Fadhil Y. Al-Aboosi, Mahmoud M. El-Halwagi, An integrated approach to waterenergy nexus in shale-gas production, Processes 6 (2018) 52, https://doi.org/ 10.3390/pr6050052.
- [52] Jamileh Fouladi, Patrick Linke, Sustainable industrial water and energy nexus integration for an industrial park, Comput. Aided Chem. Eng. 44 (2018) 1981–1986, https://doi.org/10.1016/B978-0-444-64241-7.50325-6.
- [53] Dhabia M. Al-Mohannadi, Patrick Linke, Nialy Sah, A multi-objective multi-period optimization of carbon integration networks in industrial parks, Comput. Aided

- Chem. Eng. 46 (2019) 487–492, https://doi.org/10.1016/B978-0-12-818634-
- [54] Negar Vakilifard, Martin Anda, Parisa A. Bahri, Goen Ho, The role of water-energy nexus in optimising water supply systems – review of techniques and approaches, Renew. Sust. Energ. Rev. 82 (2018) 1424–1432, https://doi.org/10.1016/j. rser.2017.05.125.
- [55] Andres Gonzalez-Garay, Gonzalo Guillén-Gosálbez, Framework for the optimal design of sustainable processes incorporating data envelopment analysis, Comput. Aided Chem. Eng. 44 (2018) 1711–1716, https://doi.org/10.1016/B978-0-444-64241-7.50280-9.
- [56] Aihua Zhu, Panagiotis D. Christofides, Yoram Cohen, Energy consumption optimization of RO membrane desalination subject to feed salinity fluctuation, Ind. Eng. Chem. Res. 48 (2009) 9581–9589, https://doi.org/10.3182/20090712-4-TR-2008.00039.
- [57] Aihua Zhu, Anditya Rahardianto, Panagiotis D. Christofides, Yoram Cohen, Reverse osmosis desalination with high permeability membranes — cost optimization and research needs, Desalin. Water Treat. 15 (2010) 256–266, https://doi.org/10.5004/dwt.2010.1763.
- [58] Md Tanvir Sowgath, Iqbal M. Mujtaba, Design of reverse osmosis process for the purification of river water in the southern belt of bangladesh, Chem. Eng. Trans. 61 (2017) 1159–1164, https://doi.org/10.3303/CET1761191.
- [59] Zhao Yu, James S. Taylor, Shankar Chellam, Predicting RO/NF water quality by modified solution diffusion model and artificial neural networks, J. Membr. Sci. 263 (2005) 38–46. URL: https://doi.org/10.1016/j.memsci.2005.04.004.
- [60] J.G. Wijmans, R.W. Baker, The solution-diffusion model: a review, J. Membr. Sci. 107 (1995) 1–21, https://doi.org/10.1016/0376-7388(95)00102-I.
- [61] Fazilet Maskan, Dianne E. Wiley, Lloyd P.M. Johnston, David J. Clements, Optimal design of reverse osmosis module networks, AIChE J. 46 (2000) 946–954, https://doi.org/10.1002/aic.690460509.
- [62] Wolfgang Marquardt, Alexander Mitsos, Notes & References for Applied Numerical Optimization (18/19), URL: https://www.avt.rwth-aachen.de/go/id/itvd/lidx/1, 2018
- [63] Carlos A. Henao, Christos T. Maravelias, Surrogate-based process synthesis, in: 20th European Symposium on Computer Aided Process Engineering – ESCAPE20, 2010, pp. 1129–1134, https://doi.org/10.1016/S1570-7946(10)28189-0.
- [64] Shawn Dorn, Saqib Shirazi, Visit H2Oaks desalination plant and information exchange. in: Tour H2Oaks Desalination Plant. 05/14/2019.
- [65] Manish Kumar, Samer S. Adham, William R. Pearce, Investigation of seawater reverse osmosis fouling and its relationship to pretreatment type, Environ. Sci. Technol. 40 (2006) 2037–2044. https://doi.org/10.1021/es0512428.
- [66] Marian G. Marcovecchio, Pio A. Aguirre, Nicolas J. Scenna, Global optimal design of reverse osmosis networks for seawater desalination: modeling and algorithm, Desalination 184 (2005) 259–271, https://doi.org/10.1016/j.desal.2005.03.056.
- [67] Consolidated Water Co. Ltd, Costs of membrane and pressure vessel units, in: Membrane Lifetime Expectancy, 07/17/2019, Phone Call.
- [68] Lilian Malaeb, George M. Ayoub, Reverse osmosis technology for water treatment: State of the art review, Desalination 267 (2011) 1–8, https://doi.org/10.1016/j. desal.2010.09.001.
- [69] Kusum Deep, Krishna Pratap Singh, M.L. Kansal, C. Mohan, A real coded genetic algorithm for solving integer and mixed integer optimization problems, Appl. Math. Comput. 212 (2009) 505–518, https://doi.org/10.1016/j.amc.2009.02.044.

- [70] Ruth Misener, Christodoulos A. Floudas, Antigone: algorithms for continuous/ integer global optimization of nonlinear equations, J. Glob. Optim. 59 (2014) 503–526, https://doi.org/10.1007/s10898-014-0166-2.
- [71] Michael R. Bussieck, Stefan Vigerske, MINLP Solver Software, Wiley Encyclopedia of Operations Research and Management Science, 2011, https://doi.org/10.1002/ 9780470400531_eorms0527
- [72] TWDB, 2017 State Water Plan: Water for Texas, URL: https://www.twdb.texas.gov/waterplanning/swp/2017/index.asp, 2017.
- [73] T. Pick, Assessing Water Quality for Human Consumption, Agriculture, and Aquatic Life Uses, Environment Technical Note No. MT-1 (Rev. 2) volume 1, United States Department of Agriculture, Natural Resources Conservation Service, Washington, DC, USA, 2011, p. 31.
- [74] Guy Fipps, Irrigation Water Quality Standards and Salinity Management Strategies, 2003, College Station (Texas). URL: http://hdl.handle.net/1969.1/87829.
- [75] Electric Power Research Institute (EPRI), Palo Alto, CA and California Energy Commission, Sacramento (California), EPRI 1005359, Use of degraded water sources as cooling water in power plants, URL: http://mydocs.epri.com/docs/A dvancedCooling/BR_EnergyWaterPubs_Final_2008-07_1016965.pdf, 2003.
- [76] San Antonio Water System, 2017 Water Management Plan, URL: https://www.saws.org/your-water/new-water-sources/2017-water-management-plan/, 2017.
- [77] San Antonio Water System, Medina lake, 10/09/2019, URL: https://www.saws.or g/your-water/new-water-sources/current-water-supply-projects/medina-lake/.
- [78] U.S. Energy Information Administration, Texas Electricity Profile 2018, URL, https://www.eia.gov/electricity/state/texas/, 2018.
- [79] Lower Colorado River Authority, Sim Gideon Power Plant, URL: https://web.archive.org/web/20060104034645/http://www.lcra.org/energy/simgideon.html, 2006.
- [80] Ashlynn S. Stillwell, Carey W. King, Michael E. Webber, Ian J. Duncan, Amy Hardberger, The Energy-Water Nexus in Texas, Ecology and Society 16, 2011. URL: http://www.ecologyandsociety.org/vol16/iss1/art2/.
- [81] Thomas M. Missimer, Noreddine Ghaffour, Abdullah H.A. Dehwah, Rinaldi Rachman, Robert G. Maliva, Gary Amy, Subsurface intakes for seawater reverse osmosis facilities: capacitylimitation, water quality improvement, and economics, Desalination 322 (2013) 37–51, https://doi.org/10.1016/j. desal.2013.04.021.
- [82] Yolanda Fernandez-Torquemada, Jose Miguel Gonzalez-Correa, Angel Loya, Luis Miguel Ferrero, Marta Diaz-Valdes, Jose Luis Sanchez-Lizaso, Dispersion of brine discharge from seawater reverse osmosis desalination plants, Desalin. Water Treat. 5 (2009) 137–145, https://doi.org/10.5004/dwt.2009.576.
- [83] Marcello Di Martino, Styliani Avraamidou, Efstratios N. Pistikopoulos, Superstructure optimization for the design of a desalination plant to tackle the water scarcity in Texas (USA), Comput. Aided Chem. Eng. 48 (2020) 763–768, https://doi.org/10.1016/B978-0-12-823377-1.50128-2.
- [84] National Centers for Environmental Information, Gulf of mexico data atlas, 2019, URL: https://www.ncei.noaa.gov/maps/gulf-data-atlas/atlas.htm.
- [85] TWDB, Carrizo-Wilcox Aquifer: Summary, URL: https://www.twdb.texas.gov/groundwater/aquifer/majors/carrizo-wilcox.asp, 2019.
- [86] San Antonio River Authority, Environmental science data, 2019, URL: https://wqdata.sara-tx.org/basin-data/?id=14195.
- [87] Martin B. Miller, Industrial Compliance Supervisor, San Antonio Water System, Available data concerning waste or brackish water: E-Mail Exchange, 05/02/2019.